Graphene-based materials for supercapacitor electrodes − A review

Qingqing Ke*, John Wang

Department of Materials Science and Engineering, Faculty of Engineering, National University of Singapore, Singapore 117574, Singapore

Abstract

The graphene-based materials are promising for applications in supercapacitors and other energy storage devices due to the intriguing properties, *i.e.*, highly tunable surface area, outstanding electrical conductivity, good chemical stability and excellent mechanical behavior. This review summarizes recent development on graphene-based materials for supercapacitor electrodes, based on their macrostructural complexity, *i.e.*, zero-dimensional (0D) (e.g. free-standing graphene dots and particles), one-dimensional (1D) (e.g. fiber-type and yarn-type structures), two-dimensional (2D) (e.g. graphenes and graphene-based nanocomposite films), and three-dimensional (3D) (e.g. graphene foam and hydrogel-based nanocomposites). There are extensive and on-going researches on the rationalization of their structures at varying scales and dimensions, development of effective and low cost synthesis techniques, design and architecturing of graphene-based materials, as well as clarification of their electrochemical performance. It is indicated that future studies should focus on the overall device performance in energy storage devices and large-scale process in low costs for the promising applications in portable and wearable electronic, transport, electrical and hybrid vehicles.
© 2016 The Chinese Ceramic Society. Production and hosting by Elsevier B.V. This is an open access article under the CC BY-NC-ND license (http://creativecommons.org/licenses/by-nc-nd/4.0/).

Keywords: Graphene-based materials; Two-dimensional materials; Supercapacitors; Energy storage

Contents

1. Introduction

Supercapacitors or ultracapacitors have attracted considerable recent attentions due to their high power density, high charge/discharge rates, and long cycle life performance [1−3]. They are considered as one of the most promising

* Corresponding author.
    E-mail addresses: msekq2001@gmail.com (Q. Ke), msewangj@nus.edu.sg (J. Wang).
    Peer review under responsibility of The Chinese Ceramic Society.

electrochemical energy storage devices, having a potential to complement or eventually replace the batteries for energy storage applications, i.e., those for wearable and portable electronics, electrical and hybrid vehicles [4]. Based on the energy storage mechanisms, supercapacitors can be classified into to two main categories, i.e., electric double layer capacitors (EDLCs) and pseudocapacitors [5]. For EDLCs, the capacitance is originated from the accumulation of charges at the electrode-electrolyte interfaces. Therefore, controlling the specific surface area and pore size and enhancing electrical conductivity are the effective ways to achieve a high storage capacity [6]. Also, the energy storage of pseudocapacitance is realized through transferring the faradic charges between electrolyte and electrode due to the reversible multi-electron redox faradaic reactions, which generally exhibits higher specific capacitance and energy density, compared to EDLCs [7—9]. However, the poor electrical conductivity in the commonly known pseudocapacitive electrodes can restrict the Faradic reactions, therefore leading to unsatisfactory electrochemical performance and life cycles.

Graphene is the well-known two-dimensional carbon monolayers composed of all-sp^2-hybridized carbons with some of the most intriguing properties, i.e., lightweight, high electrical and thermal conductivity, highly tunable surface area (up to 2675 m^2 g^{-1}), strong mechanical strength (~1 TPa) and chemical stability [10—12]. These outstanding properties enable graphene and graphene-based materials to find applications in high performance structural nanocomposites, electronics, and environmental protection and energy devices including both energy generation and storage [13—25]. The combination of these outstanding physical, mechanical and chemical properties make graphene-based materials more attractive for electrochemical energy storage and sustainable energy generation, i.e., Li-ion batteries, fuel cells, supercapacitors, and photovoltaic and solar cells [2]. For instance, the theoretical specific capacitance of single-layer-graphene is ~21 uF cm^{-2} and the corresponding specific capacitance is ~550 F g^{-1} when the entire surface area is fully utilized [10]. However, the practical capacitive behavior of pure graphene is lower than the anticipated value due to the serious agglomeration during both the preparation and application processes. Therefore, boosting the overall electrochemical performance of graphene-based materials still remains a great challenge.

Graphene-based materials have been extensively investigated as a conducting network to support the redox reactions of transition metal oxides, hydroxides and conducting polymers. Indeed, these nanohybrid electrodes consisting of graphene and nanoparticles of transition metal oxides/hydroxides or conductive polymers show the superior electrochemical performance, as a result of the synergistic effect which graphene layers facilitate the dispersion of metal oxide/hydroxide nanoparticles, and act as a highly conductive matrix for enhancing the electrical conductivity, and the metal oxide/hydroxide/conducting polymers offer the desired pseudocapacitance.

In this review, recent development on the preparation methods, resultant structures and electrochemical performance of graphene-based materials designed for applications in supercapacitors was summarized. The corresponding capacitive mechanisms and the effective ways to achieve high energy storage performance were also discussed.

2. Graphite, graphite oxides, and graphene

Graphite is a well known natural mineral [26], which is highly anisotropic in both structure and functional behavior, with the in-plane electrical and thermal conductivities being 1000-fold greater than those in the out-of-plane direction. Similarly, the in-plane strength and modulus of graphite are much greater than those of the out-of-plane due to the different types of bonds in the two directions. Some techniques of producing graphite of different qualities in large scales are used, graphite is thus one of the most widely used materials in various structural, functional, chemical and environment applications. This material is also used in energy storage applications. Mitra et al. developed solid-state electrochemical capacitors by using graphite as electrodes, where the calculated specific capacitances were in the range from 0.74 to 0.98 mF cm^{-2}, together with a long cycle life and a short response time [27].

Graphene is the monolayer of graphite, which can be prepared by several techniques. Geim et al. prepared graphene from graphite and demonstrated an experimental method to prepare a single layer of graphite with thickness in atomic scale, named as graphene. Since then graphene has become popular in various application aspects due to its inherently superior electrical/electronic and optical properties (i.e., tunable bandgap, extraordinary electronic transport behavior, excellent thermal conductivity, high mechanical strength and largely tunable surface area) [28]. Also, some chemical and physical techniques for synthesis of graphene have been developed. Graphene oxides (GO) are another important member in the graphene—graphite family, which are considered as derivatives of graphene. They that can be readily made from graphite, exhibit the layered structure and the surface-related properties [32,33]. Depending on the synthesis techniques, there can be different surface groups in graphene oxides as well as their distributions on the surface. For instance, the oxygen-containing functional groups (hydroxyl (C—OH), carboxyl (C=O) and epoxy groups (C—O)) locate around the edges of graphene sheets and stabilize the quasi-two-dimensional sheets. Graphene oxides can be readily converted into graphene by different reduction processes. Fig. 1 shows the reduction of graphene oxide (GO) by both thermal method and reducing agents [34,35]. As a precursor for graphene, GO can be easily derived from the oxidation of natural graphite at a large scale and low costs. The reduction of GO is a low-cost technique for producing graphene [36]. The atomic layers of GO generally comprises phenol epoxy and epoxide groups on the basal plane and ionizable carboxylic acid groups around the edges [37,38]. The acid groups on the ionized edge enable the stabilization of GO in aqueous

dispersion in the form of a single-sheet layer through weak dipole and quadrupole van der Waals interaction in the surrounding environment. This makes GO a high degree of processing and dispersion ability in solution, and offers the desired convenient method for producing graphene-based materials in a large scale.

For both energy storage and other applications, some research work are dedicated to the synthesis of graphene sheets, where the generally facile approaches can be divided into the following categories: i) epitaxial growth and chemical vapor deposition (CVD) of graphene on substrates, such as SiC and matched metal surfaces [39,40]; ii) mechanical cleavage of graphite, for instance, using atomic force microscopy (AFM) cantilevers or even adhesive tapes [29]; iii) chemical exfoliation of graphite in organic solvents [30]; iv) gas-phase synthesis of graphene platelets in microwave plasma reactor [41]; v) synthesis of multi-layered graphene by arc-discharge [42]; and vi) reduction from GO derived from the oxidation of natural graphites in a large scale [36]. Among these production methods, graphene prepared by CVD offers the better properties, as a result of their large crystal domains, monolayer structure and less defects in the graphene sheets, which are beneficial for boosting carrier mobility in electronic applications [26]. In addition to mechanical exfoliation by adhesive tapes, Firsov et al. demonstrated the mechanical cleavage of graphite using atomic force microscopy (AFM) cantilevers [29]. Mechanical exfoliation is, however, associated with a low yield, therefore generally restricting the mass production of graphene. Hernadez et al. developed chemical methods to exfoliate graphite in organic solvents [30]. Therefore, the production of graphene at a low cost, a high yield and a high quality have been taken into account in recent years. In general, the chemical exfoliation of graphite into GOs, followed by controllable reduction of GOs (with reduction agent such as hydrazine hydrate) into graphene is believed to be the most efficient and low-cost method [43]. Although individual graphene sheets are often partially agglomerated into particles of approximately 15−25 μm in diameter during the reduction process, the product with high specific surface areas of a few hundreds $m^2 g^{-1}$ can be obtained, offering an electrode material of energy storage devices for the potential application (see Fig. 2).

Ruoff et al. pioneered the chemically modified graphene (CMG) as electrode materials [44]. They found that the specific capacitances of 135 and 99 F g^{-1} could be achieved in aqueous and organic electrolytes, respectively. Ajayan et al. reported a two-step method to fabricate a highly reduced GO via deoxygenation with $NaBH_4$ and dehydration with concentrated sulfuric acid [45]. The comb-like connected sheet structure needs to be protected during the harsh oxidation and reduction process in order to maintain the performance. To reduce the level of toxicity of the reduction agents, there are some efforts to prepare graphene with non-toxic agents. Zhu et al. synthesized graphene using sugar as a reduction agent. Zhang et al. employed ascorbic acid [46,47]. In addition, "green" materials of melatonin vitamin C, bovine serum albumin, polyphenols of green tea and even bacterial respiration were also proposed to produce reduced graphene oxides (rGO) [48−54]. Similarly, "green" methods, i.e., the flash photo reduction of GO into graphene, solvothermal reduction, hydrothermal dehydration, catalytic reduction and photo catalytic reduction were reported [55−63]. In particular, one-step hydrothermal method is a versatile and low-cost process to produce the rGO. Shi. et al. reported the reduction of GO via the one-step hydrothermal approach. The rGO thus shows a high conductance of 5×10^{-3} S cm^{-1} and a high specific capacitance of 175 F g^{-1} with aqueous electrolyte. Nevertheless, it is rather challenging to completely reduce GO as some of the oxygen-containing surface groups are rather difficult to be eliminated [6].

3. Graphene-based supercapacitor electrode materials

Graphene can be assembled into several different structures, i.e., the free-standing particles or dots, one-dimensional fibers or yarns, two-dimensional films and three-dimensional foams and composites. Recent studies focus on graphene-based electrode materials according to their macrostructural complexity, i.e., zero-dimensional (0-D) (e.g. free-standing graphene dots and particles), one-dimensional (1-D) (e.g. fiber-type and yarn-type structures), two-dimensional (2-D) (e.g. graphenes and graphene-based films), and three-dimensional (3-D) (e.g. graphene foams and composites).

3.1. Graphene dots and powders as supercapacitor electrodes

Graphene dots and particles can be made through chemical exfoliation of graphite into GO, followed by controllable reduction of GO (with reduction agent such as hydrazine
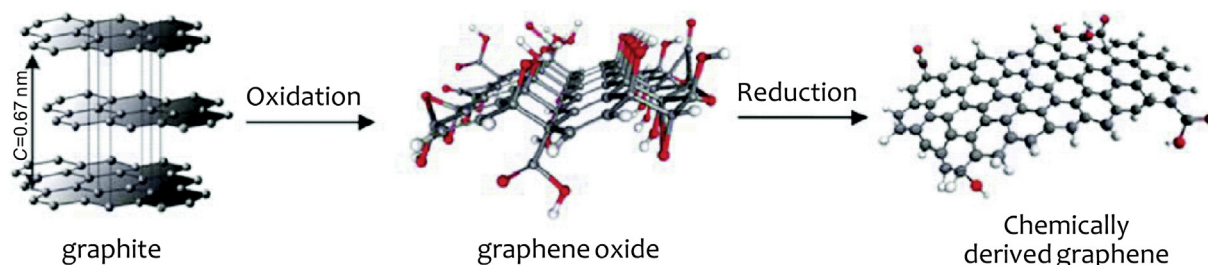

Fig. 1. Illustration of the chemical route to the chemically derived graphene [31]. Copyright 2009, Rights Managed by Nature Publishing Group.
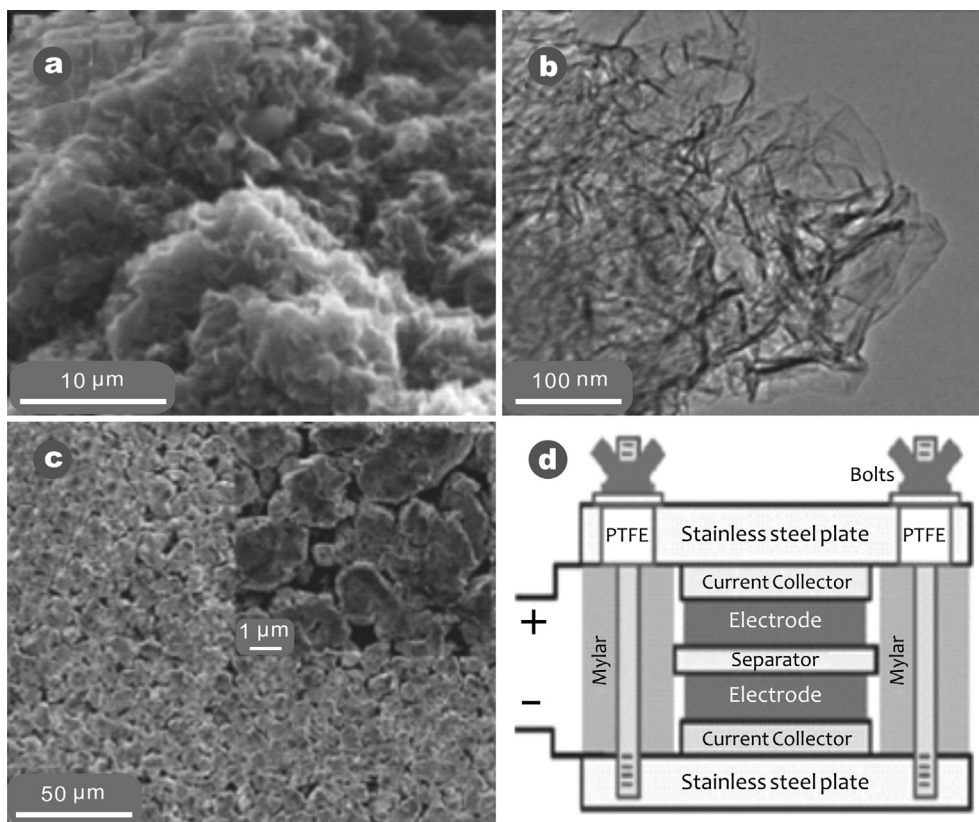
Fig. 2. Graphene-based supercapacitors. (a) SEM image of CMG particle, (b) TEM image showing individual graphene sheets extending from the CMG particles, (c) low and high- (inset) magnification SEM images of CMG particles electrode, and (d) schematic of test assembly. Reproduced with permission [44]. Copyright 2008, American Chemical Society.

hydrate). The resultant graphene particles are readily agglomerated and the rGO becomes hydrophobic by the subsequent reduction, which affect further processing in water or aqueous environment. In contrast, GO is a unique amphiphile with negative charged hydrophilic edges and hydrophobic basal plane [64]. This unique character allows GO to selectively interact with certain surfactants, which are capable of tuning the amphiphilicity of GO and controlling the assembly of rGO. Zhang et al. investigated the surfactant-stabilized graphene-based materials with different surfactants like tetrabutylammonium hydroxide (TBAOH), cetyltrimethylammonium bromide, and sodium dodecylbenzene sulfonate [65,66]. They found that the rGO sheets could be intercalated by the surfactants. The specific capacitance of 194 F g^{-1} was obtained from the TBAOH stabilized graphene as a supercapacitor electrode at the current density of 1 A g^{-1}, which was partially contributed to a decreased degree of rGO re-stacking and increased wettability in the presence of the surfactant intercalation. In addition, the modification by surfactant can homogeneously disperse rGO into single or a few layers in aqueous solutions. These properties permit chemical reactions between rGO and second phases in the aqueous solvents. Among many surfactants investigated, commercially available block copolymers poly-(ethylene oxide)-poly (phenylene)-poly (ethylene oxide) PEO$_{106}$-PPO$_{70}$-PEO$_{106}$ (F127) were widely investigated due to their well-established

chemical behaviors [67]. Also, such block copolymers can self-assemble through hydrogen bonding and hydrophobic−hydrophilic interactions in aqueous environments to form vesicles, which can be used as soft templates for fabricating mesoporous carbon materials [68,69]. Ke et al. intercalated GO with triblock copolymer Pluronic F127 (F127) in hydrothermal process, followed by thermal annealing to realize the structural reconstruction. In their work, a specific surface area of 696 m^2 g^{-1} is achieved in the surfactant-modified graphene, which is about three times greater than that of pristine graphene (*i.e.*, 200 m^2 g^{-1}). A maximum specific capacitance of 210 F g^{-1} was measured at a scanning rate of 1 mV s^{-1} in 6 M KOH electrolyte, together with superior cycling stability (*i.e.*, 95.6% of the initial capacity remained after 1000 cycles) [35].

Although supercapacitor electrodes made of graphene powders generally show a high power density due to the high surface area and good electrical conductivity, they are a fast charge transfer [70,71]. They are limited by the modest capacitance value (~200 F g^{-1}). Therefore, the energy density and overall device performance are generally unsatisfied. In contrast, the pseudocapacitance derived from some of the transition metal oxides (*i.e.*, MnO$_2$, RuO$_2$, NiO, Co$_3$O$_4$ and Fe$_3$O$_4$) or hydroxides (Ni(OH)$_2$ and Co(OH)$_2$), as well as electrically conductive polymers (*i.e.*, PANI, polypyrroles, and polythiophenes), as a result of the reversible faradaic redox

reactions at the electrode surface, shows a higher specific capacitance. Carbon-based materials, i.e., graphene, are the key electrode materials in EDLCs [72−76]. To effectively synergize the EDLC and pseudocapacitance, one way is to develop hybrid electrodes by integrating the metal oxides/hydroxides or conductive polymers with graphene network. In the hybrid electrodes, graphene will function as a conductive channel for charge transfer and therefore improve the overall conductivity, while pseudocapacitance arises from the metal oxides/hydroxides or conductive polymers [6].

Among the composites with metal oxides, graphene-MnO_2 composites were widely investigated [77−80]. Yang et al. devised a simple approach to prepare hydrothermally reduced graphene-MnO_2 composites. Their experimental results show that the graphene-MnO_2 composite powders exhibit a specific capacitance value of 211.5 F g^{-1} at the potential scan rate of 2 mV s^{-1} and with about 75% capacitance being retained after 1000 charge/discharge cycles in 1 M Na_2SO_4 electrolyte [81]. Dai et al. synthesized $Ni(OH)_2$ nanoplates on graphene sheets. The hybrid electrode material exhibits a high specific capacitance of ~1335 F g^{-1} at the charge and discharge current density of 2.8 A g^{-1} and ~953 F g^{-1} at 45.7 A g^{-1}, and high power density and energy density [82]. These graphene-based metal oxide/hydroxide composites were prepared *via* reduction of GO, and followed by the loading of pseudocapacitive materials. However, the superior electric and surface properties of graphene may not be fully utilized due to the unexpected agglomerations [83]. For instance, exfoliated GO sheets possess a high surface area, which tend to be restacked. To improve the potential of graphene sheets, a strategy is to properly load some of the oxide/hydroxide nanocrystals on the graphene surface, which will have the dual functions of providing pseudocapacitance as well as spacers between the graphene layers. Ke et al. reported a facile method of synthesizing Fe_3O_4-rGO nanocomposite powders *via* the electrostatic interaction between Fe_3O_4 nanoparticles and GO and the subsequent reduction of GO into rGO by a hydrothermal method [84]. This nanocomposite powder shows an improved specific capacitance of 169 F g^{-1} in 6 M KOH electrolyte, which is much greater than that of Fe_3O_4 (68 F g^{-1}) at the current density of 1 A g^{-1}. This intercalated hierarchical nanocomposite powder also demonstrates a good capacitance retention, retaining over 88% of the initial capacity after 1000 cycles. Similarly, Wu et al. developed a nanocomposite consisting of well-dispersed Co_3O_4 in rGO network, directly derived from GO-$Co(OH)_2$, followed by thermal treatment. The nanocomposite electrodes have a specific capacitance of 291 F g^{-1} at 1 A g^{-1} in the potential range of −0.4−0.55 V in 6 M aqueous KOH solution, and the superior rate capability and cycling ability [83].

Although the chemical reduction approach for graphene is an efficient and low-cost method to produce graphene in a relatively large scale, the materials derived exhibit a moderate electrical conductivity and general lack of micro-pores, which are required for electrochemical energy storage. Accordingly, there have been efforts to improve the electrical conductivity and specific surface area [85]. In this case, some template-assisted processes were developed. Yoon et al. devised a template-directed process to synthesize hollow graphene balls (GBs) using Ni nanoparticles as a template. In this method, a carburization process was used to facilitate carbon transport into Ni-NPs with a polyol solution, and a thermal annealing process was then used to stimulate carbon segregation, therefore resulting in graphene layer formation on the surfaces of Ni-NPs. The GBs thus derived maintain their spherical shapes and dispersive during the thermal annealing process, even after removal of the core template of Ni-NPs, yielding hollow GBs composed of multilayer graphene [86]. Similarly, Lee et al. developed a mass-producible mesoporous graphene nanoball (MGB) *via* a precursor-assisted chemical vapor deposition (CVD) technique for supercapacitor application [85]. Fig. 3 shows the morphological development of the polymeric spheres and MGB prepared by the precursor-assisted CVD method. In Fig. 3a, SPS-COOH spheres with a diameter of around 250 nm are nearly uniform in size and morphology. In Fig. 3c and d, the mesoporous graphene nanospheres with a mean pore diameter of 4.27 nm are formed. The MGB is mesoporous with a mean mesopore diameter of 4.27 nm and a specific surface area of 508 m^2 g^{-1}. The supercapacitor device made of MGB as the electrode demonstrates a specific capacitance of 206 F g^{-1} and more than 96% retention of capacitance after 10,000 cycles. More recently, Park, et al., integrated graphene nanosheets into micro/macro-sized powder structure. In their work, a spray-assisted self-assembly process was used to prepare spherically integrated graphene microspheres by using a high-temperature organic solvent in a manner reminiscent of deep-frying. The resultant supercapacitor electrode demonstrates an electrochemical performance of 151 F g^{-1} at the scan rate of 10 mV s^{-1} [87].

3.2. 1D graphene-based fibers and yarns

Graphene-based fibers and yarns have a great application potential due to the combined merits of tiny volume, high flexibility and weave-ability, which promise some applications in the next generation supercapacitors for wearable and portable devices and electrical vehicles [88]. The carbon-based materials, i.e., carbon fibers, CNTs, graphene and mesoporous carbon can be made into various fiber and yarn forms. They can be also hybrided with selected electrical active materials with faradaic pseudocapacitance, i.e., metal oxides, hydroxides and conducting polymers (e.g., polypyrrole, PANI, poly(3,4-ethylenendioxythiophene, PEDOT) [89−92].

A solid electrochemical capacitor made of fiber-shaped rGO coated on Au wires was reported, exhibiting a high specific capacitance of 101.9 uF cm^{-1} (6.49 mF cm^{-2}) with a rather small capacitance loss (lower than 1%), even when is bent to 120° or twisted into an S-shaped structure. To achieve a lighter electrode material, Meng et al. developed an all-graphene yarn supercapacitor, where Au wires as a core were replaced with rGO and a sheath of graphene was electrochemically deposited onto the graphene framework. The
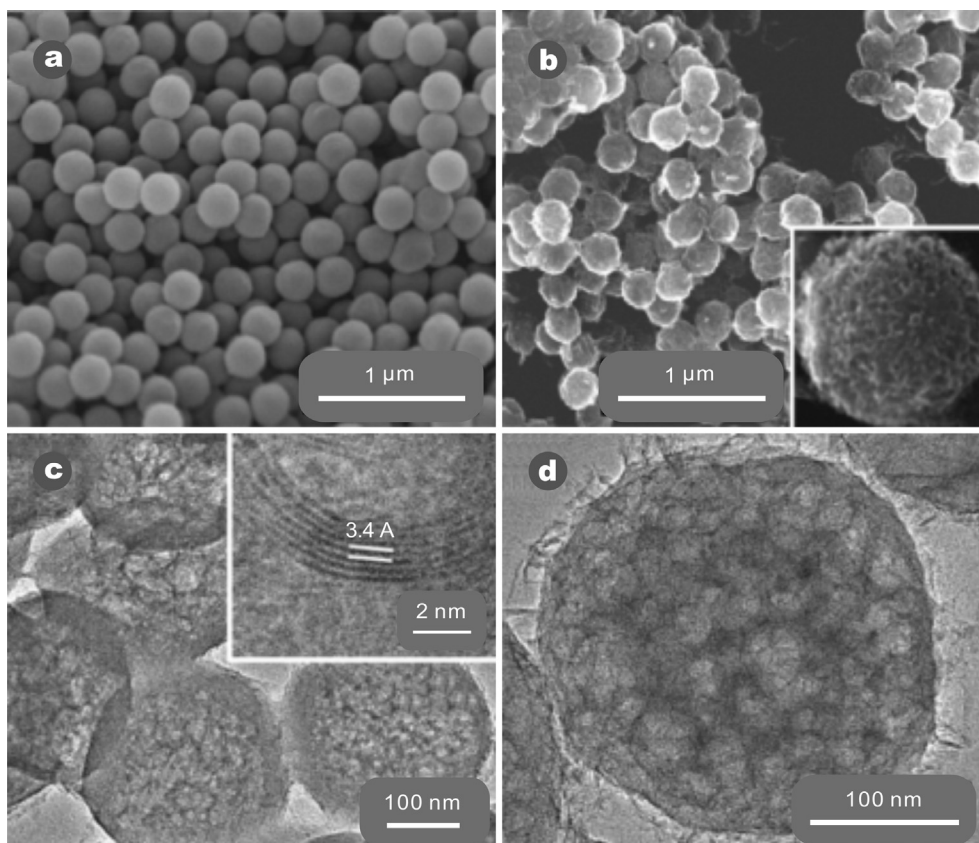
Fig. 3. SEM images of (a) SPS-COOH, and (b) MGB obtained by CVD of sample (a). The inset in panel b shows the close-up SEM image of mesoporous single graphene ball. (c) TEM images of MGB taken near the edges of the sample. The inset confirms ~7 layers of MGB with an interlayer spacing of 0.34 nm. (d) Magnification image of a single graphene ball with meso-pores [85]. Copyright 2013, American Chemical Society.

graphene fibers (GFs) produced show a density of 0.23 g cm^{-3}, which is 7 times and 85 times lower than that of conventional carbon fibers (>1.7 g cm^{-3}) and Au wire (ca. 20 g cm^{-3}), respectively [88]. The all-graphene yarns exhibit a high electrical conductivity and a great surface area due to the 3D interpenetrating porous networks of graphene. The solid state of such materials made of all graphene fibers using H$_2$SO$_4$-PVA gel electrolyte could be processed to spring-shaped supercapacitors, which possess highly compressible and stretchable mechanical performance and show an areal capacitance of 1.2−1.7 mF cm^{-2} [93]. Although the resultant graphene fibers are light-weight, highly flexible and electrically conductive, the restacking interaction between individual graphene sheets dramatically lower the large initial surface area of graphene sheets. Recent studies showed that hybrid materials combining 2D graphene sheets with 1D CNTs have a synergistic effect with greatly improved electrical, thermal conductivities and mechanical flexibility, compared to either of the single component alone. Cheng et al. developed hybrid fibers (CNT-G) by CVD growth of one-dimensional (1D) carbon nanotubes (CNTs) on 2D graphene. The CNT-graphene hybrid fibers prepared exhibit an areal capacitance of 1.2−1.3 mF cm^{-2} with a stable CV performance even after 200 bending cycles in the textile structures [94]. The above-mentioned yarn supercapacitors are, however, "naked" and thus are easy to be short-circuited when contacted with each other, even with post-coating a layer of poly(vinyl alcohol) (PVA) solid electrolyte. Kou et al. designed a coaxial wet-spinning assembly process to fabricate polyelectrolyte-wrapped graphene-CNT core-sheath fibers continuously (see Fig. 4). The sheath layer of the polyelectrolyte effectively avoids the risk of the short circuit. The maximum capacitances achieved are C$_1$ (5.3 mF cm^{-1}), C$_A$ (177 mF cm^{-2}) and C$_V$ (158 F cm^{-3}), which are ascribed to the large surface area and an efficient ion transportation between electrodes [93]. Yu et al. reported a scalable method to synthesize hierarchically structured carbon microfibers, which are made of single-walled carbon nanotubes (SWNT)/nitrogen-doped rGO with a superior electrical conductivity (*i.e.*, 102 S cm^{-1}) and a great surface area (*i.e.*, 396 m^2 g^{-1}). The resultant fiber-typed supercapacitor shows a specific volumetric capacity of 305 F cm^{-3} in sulfuric acid (measured at 73.5 mA cm^{-3} in three-electrode cell) or 300 F cm^{-3} in polyvinyl alcohol (PVA)/H$_3$PO$_4$ electrolyte (measured at 26.7 mA cm^{-3} in two-electrode cell). Furthermore, a full micro-supercapacitor with PVA/H$_3$PO$_4$ gel electrolyte shows a volumetric energy density of ~6.3 mWh cm^{-3}. To increase the energy density, asymmetric supercapacitors based on graphene fibers were explored. Wang et al. prepared solid-state supercapacitors, in which Co$_3$O$_4$ coated Ti wires and carbon fiber-graphene were used as the anode and cathode, respectively. The operation window could be increased to 1.5 V and an improved energy
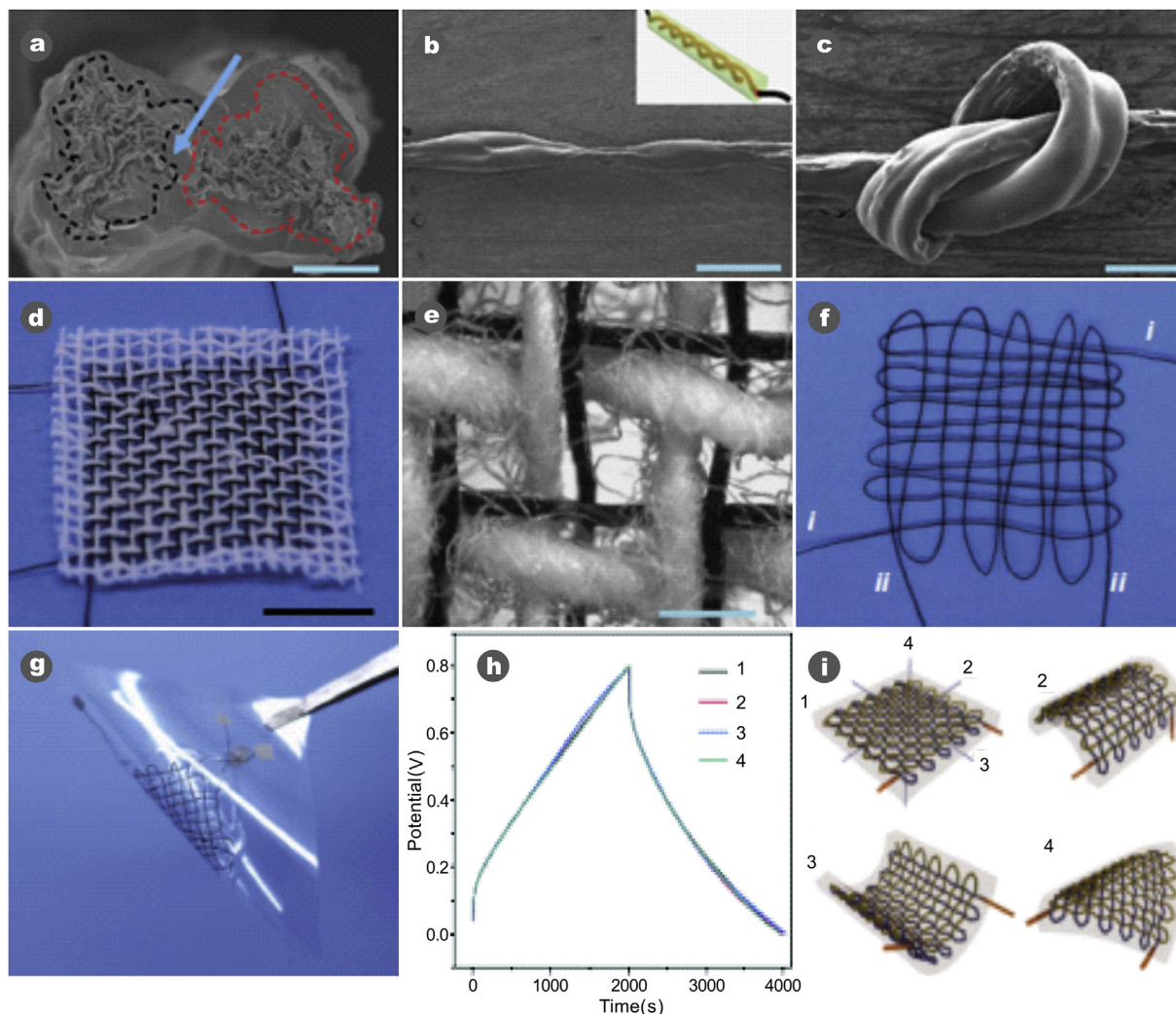
Fig. 4. Two-ply YSCs and their electrochemical properties. SEM images of cross-sectional (a), and side (b) view of a two-ply YSC. The arrow area in (a) is PVA/ H_3PO_4 electrolyte and inset of (b) shows the schematic illustration of YCS. (c) SEM image of a two-ply YSC knot. (d) Two intact coaxial fibers woven with cotton fibers. (e) Optical macroscopic image of (d). (f) cloth woven by two individual coaxial fibers. (g) supercapacitor device based on the cloth fabricated by two coaxial fibers (denoted as i and ii, respectively). (h) GCD curves of the cloth supercapacitor. (i) Scheme shows the cloth under different deformation. 1 represents initial cloth supercapacitor without bending and 2, 3, 4 show cloth supercapacitor with bending angles of 180° along three directions) [93]. Copyright 2014, Rights Managed by Nature Publishing Group.

density of 0.62 mWh cm^{-3} and power density of 1.47 W cm^{-3} [95]. MnO$_2$ coated rGO-SWCNTs and pristine rGO-SWCNTs were assembled into asymmetric electrodes, offering a high voltage window of up to 1.8 V, an improved power density (929 mW cm^{-3}) and energy density (5 mWh cm^{-3}). Recently, Seyed. et al. developed a fabrication process for highly porous GO and rGO fibers and yarns by taking the advantage of the intrinsic soft-assembly behavior of ultra-large GO liquid crystalline dispersions. The yarns derived are mechanically robust, electrically conductive and great specific surface area (i.e., 2210 m^2 g^{-1}). The architecture exhibits an open network structure with continuous ion transport pathway, therefore leading to a charge storage capacity (i.e., 409 F g^{-1} at 1 A g^{-1}) [96]. Although the yarn-type supercapacitors are of great interest due to their high flexibility and weave-ability, the bottleneck is, however, to develop a device of both high energy and power density. Liu et al. reported a hierarchical composite electrode consisting of low-cost graphene sheets immobilized onto the surfaces of Ni-coated cotton yarns, which were fabricated via scalable electroless deposition of Ni and electrochemical deposition of graphene on the common cotton yarns [97]. The supercapacitor derived yarns is highly flexible and capable of being integrated into wearable electronic devices. The device demonstrates a high volumetric energy density of 6.1 mWhcm^{-3} and a power density of 1400 mW cm^{-3}, respectively. Nevertheless, there are still some challenges for further improvement. The future work should be focused on the reduction of the unwanted restacking of graphene sheets, and the modulation of microporous structures within the graphene yarns for the development of the hierarchically structured nanocomposite electrodes.

3.3. 2D graphene film-based supercapacitors

Graphene is considered as one of the most promising materials for the next generation flexible thin film supercapacitors due to its unique structural and property features, *i.e.*, i) the two-dimensional structure can provide a large surface area, which serves as an extensive transport platform for electrolytes [98]; ii) the high conductivity of graphene sheets enables a low diffusion resistance, therefore leading to enhanced power and energy density; and iii) the superior mechanical property makes graphene sheets being easily assembled into free-standing films with robust mechanical stability. Among the graphene-based 2D films, graphene papers have attracted much attention due to the tunable thickness, structural flexibility, lightweight and electrical properties, which are the essential qualities required for flexible supercapacitors [98]. Considerable research efforts have therefore been dedicated to exploring novel processing methods for graphene-based films and papers, including spin-coating [23], Langmuir−Blodgett, layer-by-layer deposition, interfacial self-assembly, and vacuum filtration [99−101].

In a similar situation as with other graphene-based materials, the processing of graphene thin films and papers is hindered due to the agglomeration and restacking of graphene sheets resulting from the inter-planar π−π interaction and van der Waals forces, which can greatly reduce the surface areas and limit the diffusion of electrolyte ions between graphene layers [102−104]. There were numerous attempts to break the processing bottleneck, *i.e.*, adding spacers, template-assisted growth, and crumpling of the graphene sheets [105−107].

Separation by appropriate spacers is an approach effective to improve the stacking of graphene sheets. The most widely investigated spacers are carbonaceous materials (e.g., carbon particles, CNT), metals (e.g., Pt, Au) or metal oxides (e.g., SnO_2), and other pseudocapacitive materials (e.g., transitional metal oxides, hydroxides and conducting polymers) [108−111]. Wang et al. developed a flexible graphene paper incorporating with small amounts of carbon black nanoparticles as spacers between graphene sheets, which provide an open structure for charge storage and ion diffusion channels, therefore resulting in a significant improvement in electrochemical performance (*i.e.*, a specific capacitance of 138 F g^{-1} in aqueous electrolyte at the scan rate of 10 mV s^{-1} and only 3.85% capacitance being lost after 2000 cycles at the current of 10 A g^{-1}) [108]. Li et al. reported a flexible graphene film paper using CNTs as a spacer to prevent the inter sheet restacking [109]. This multilayered graphene structures enable the hybrid electrodes to have a high specific capacitance of 140 F g^{-1} at the current density of 0.1 A g^{-1} in 1 M H_2SO_4 solution. Si et al. employed the Pt as spacers to separate the graphene sheets, and they found that the Pt-separated graphene sheets exhibited a significantly enlarged capacitance of 269 F g^{-1}, compared to normal graphene with a capacitance of 14 F g^{-1} [110]. Paek et al. modified graphene sheets with SnO_2 particles, which were mixed in between the inter-sheets of graphene layers [112]. Due to the expended inner space

among graphene sheets, the capacitance is greatly improved, leading to an enhanced energy storage ability.

With the restacking of graphene sheets being tackled at least partially, the gravimetric specific capacitance of graphene films with carbon-based spacers or metal nanoparticles is improved up to ~300 F g^{-1} [26]. In order to further increase the energy density, pseudocapacitive materials with large capacitances were employed as spacers. They are several transition metal oxides and hydroxides, such as RuO_2, Fe_3O_4, CuO, $Ni(OH)_2$, MnO_2, Co_3O_4, and conductive polymers such as polyanilines (PANI), polypyrrole (PPy) and polythiophene (PT) [72,113−115].

Wang et al. reported graphene sheets intercalated with single crystalline hexagonal $Co(OH)_2$ nanoplates, which can provide the desired void space between graphene layers and contribute to the pseudocapacitance. This hybrid-type electrode material demonstrates an impressive specific capacitance of 1335 F g^{-1} at the current density of 2.8 A g^{-1} [82]. Li et al. further developed a bendable film electrode material, where $Ni(OH)_2$ nanoplates are intercalated between the densely stacked graphene sheets (GNiF) (see Fig. 5). The 3D expressway-like electrode exhibits a capacitance performance of 537 F g^{-1} and a high volumetric capacitance of 655 F cm^{-3} [116]. MnO_2 as a common pseudocapacitive material is also used to space graphene layers, which offers the environmental compatibility and low cost. Choi. et al. developed a film-type electrode by hybriding graphene with MnO_2 by a filtration method. The resultant nanocomposite film shows a specific capacitance of 389 F g^{-1} in 1 M $NaSO_4$ and the capacitance retention of 95% after 1000 cycles [117]. Yang et al. constructed an asymmetric configuration with Fe_2O_3 and MnO_2 nanoparticles being incorporated into macroporous graphene film electrodes. They found a working potential window up to 1.8 V and an energy density of 41.7 W h kg^{-1} together with a power density (13.5 kW kg^{-1}). The high energy and power density could be maintained for over 5000 cycles, even at a high current density of 16.9 A g^{-1} [118].

Besides the development of solid-spacer intercalations in graphene, solution-based spacing was also developed to reduce the agglomeration of graphene sheets. Li et al. investigated water as a "spacer" to prevent the restacking of graphene sheets [119]. The graphene-water hybrid is generated through the balance between the repulsive interaction and inter-sheet π−π attraction among the solvated graphene layers. It is self-stacked into graphene film rather than restacked into the graphite structure. The solvated graphene film is demonstrated with a high specific capacitance of 215 F g^{-1} and a good retention ability, where the capacitance of 156.5 F g^{-1} can be retained at a high current density of 1080 A g^{-1} and >97% cycling ability being retained after 10,000 cycles at the current density of 100 A g^{-1}. The solution-based spacing approach can be extended to other types of liquids. Park et al. functionalized graphene with Nafion and assembled the functionalized graphene into films [120]. Nafion being an amphiphilic molecule prevents the aggregation of graphene sheets and improves the interfacial wettability between electrode and electrolytes, therefore
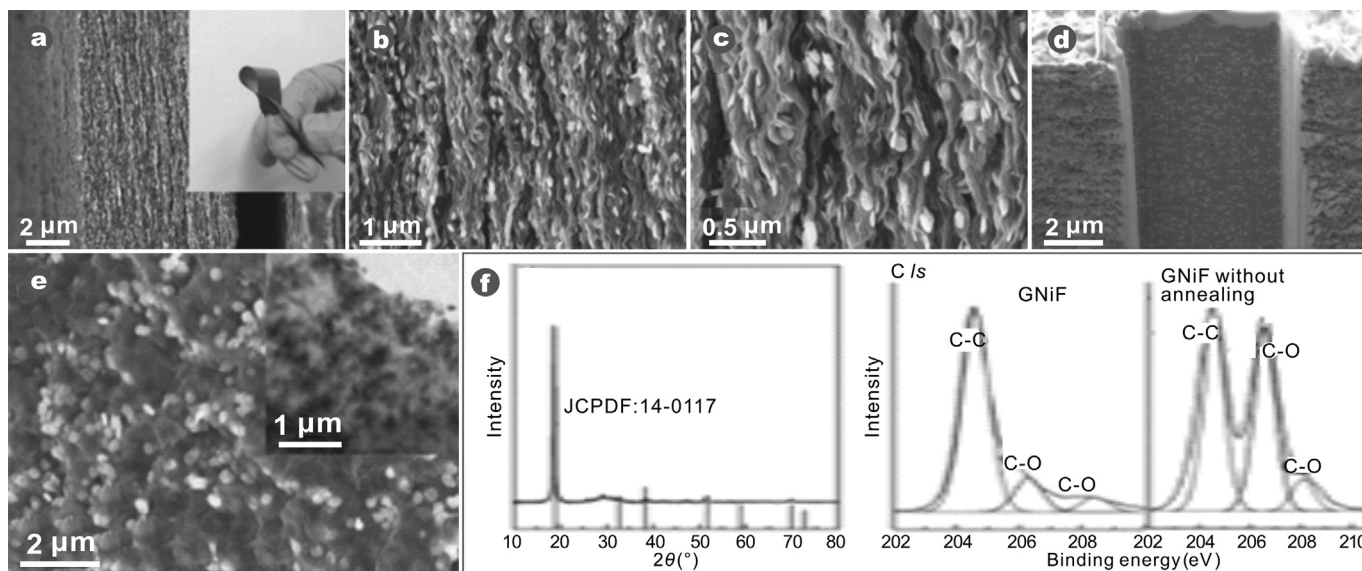
Fig. 5. Morphologies and structure characterization of graphene film intercalated with Ni(OH)$_2$ nanoplates. (a)−(c) cross sectional SEM images of the GNiF at different magnifications, inset optical images of the GNiF showing its flexibility, (d) side view of foccused-ion beam-etched GNiF in parallel direction to the graphene sheets, (e) in-plane viewed SEM and TEM (inset) of GNiF in perpendicular direction to the graphene sheets, (f) XRD pattern and XPS carbon core level XPS spectra of GNiF [116]. Copyright 2014 Wiley-VCH Verlag GmbH & Co. KGaA, Weinheim.

promoting fast ion transports. The Nafion modified graphene film shows a specific capacitance of 118.5 F g^{-1}, which is two times greater than that of pristine rGO film, and 90% retention can be achieved at the high current density of 30 A g^{-1} [97]. Li et al. developed a flexible, porous and yet densely packed graphene gel film (CCG) via the capillary compression of chemically converted graphene in the presence of volatile and nonvolatile liquid electrolytes (see Fig. 6) The packing density of such a graphene film is nearly doubled (~1.33 g cm^{-3}) in contrast to that of the traditional porous carbons. It has a volumetric capacitance of 255.5 F cm^{-3} with aqueous electrolyte [102].

Graphene sheets intercalated with conducting-polymer also attract much interest [121,122]. Cheng et al. reported a fabrication process to prepare graphene-PANI composite paper by using in-situ anodic elelctropolymerization of aniline monomer on graphene paper. The hybrid type film presents a gravimetric capacitance of 233 F g^{-1} and a volumetric capacitance of 135 F cm^{-3} [123]. Similarly, Wei et al. synthesized a graphene-PANI composite by a polymerization method, where graphene (~15 wt %) was homogeneously coated on to PANI sheets [124]. A specific capacitance of 1046 F g^{-1} was measured, and 96% of capacitance value was maintained even when the current density increased from 10 to 100 A g^{-1}, indicating a superior retention ability [125]. Zhang et al. devised a graphene-based film by intercalating PPy spheres between graphene layers, therefore creating a desired hollow structure. This nanocomposite film-type electrode demonstrated enhanced electrochemical performance with a capacitance value of 500 F g^{-1} at the charging−discharging current density of 5 A g^{-1} [126]. Wang et al., prepared polyaniline (PANI) nanowire arrays on flexible polystyrene microsphere/reduced graphene (PS/rGN) film via dilute polymerization and then PS microspheres being removed to

form free-standing rGN/PANI nanocomposite film [127]. The nanowire array structure significantly increases the active surface area of electrode and provides a high interfacial area
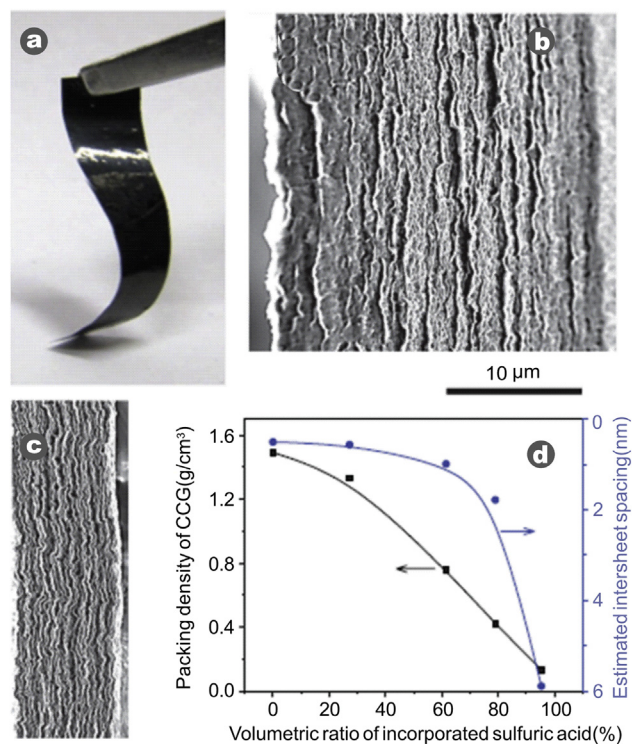

Fig. 6. Characterization of liquid electrolyte-mediated CCG film: (a) A photograph showing the flexibility of the film. (b) and (c) SEM images of cross sections of the obtained EM-CCG films containing (b) 78.9 volume percent (vol. %) and (c) 27.2 vol. % of H$_2$SO$_4$, respectively. (d) The relation between the volumetric ratio of incorporated electrolyte and the packing density as well as the estimated inter sheet spacing [102]. Copyright 2013, American Association for the Advancement of Science.

and shortens ion diffusion paths. A specific capacitance of 740 F g^{-1} (or 581 F cm^{-3}) was achieved at the current density of 0.5 A g^{-1}. The specific capacitance retains 87% of the initial value after 1000 charge−discharge cycles at the current density of 10 A g^{-1}. Moreover, a maximum energy density of 65.94 W h kg^{-1} was obtained at the power density of 0.2 kW kg^{-1}. PEDOT [poly (3,4-ethlenediolxythiophene)] as well as its derivatives were investigated, which were known to possess high electrical conductivity, chemical and thermal stability and electrochemical behavior in a relatively wide potential window [128,129]. Lehtimäki et al., demonstrated that PEDOT and GO can be combined by a simple electro-polymerization process on flexible substrates, and GO be further reduced *via* electrochemical reduction to rGO [130]. The device made of PEDOT/rGO was shown with a capacitance of 14 F cm^{-2}, which was ascribed to the largely accessible surface area of rGO combined with the pseudoca-pacitance of PEDOT.

3.4. 3D graphene-based electrodes materials

As mentioned above, graphene-based nanocomposite films incorporating guest nanoparticles into 2D graphene sheets can favor the reduction of graphene aggregation, which are otherwise limited by ion access to the overall 2D structure [131]. To further address this and other related issues, considerable efforts were made to develop graphene-based macrostructures with 3D networks, *i.e.*, aerogels, graphene

foams, and sponges [132−136]. These 3D graphene-based materials, consisting micro- meso- and macro-interconnected pores, high surface areas and fast ion/electron transport channels, are highly desirable for exploring both high energy and power density, and overall supercapacitance performance [97,137−142]. Indeed, some of these 3D graphene-based structures showed outstanding electrochemical behavior for energy storage, as well as other functional properties such as mechanical and catalytic properties [143].

Several processing techniques were reported for the prep-aration of the 3D graphene-based supercapacitor electrodes. For instance, a template-directed assembly technique was developed to fabricate 3D macroporous bubble graphene foam. Cheng et al. used monodisperse polymethyl methacry-late (PMMA) spheres as hard templates, which were then removed *via* calcination at 800 °C [144]. The resultant 3D bubble graphene structure provides controllable and rather uniform macropores and tailorable overall microstructure, therefore leading to a high capacitance retention of 67.9% with increasing a scanning rate up to 1000 mV s^{-1} (see Fig. 7). However, the annealing procedure at high temperature (*i.e.*, ~800 °C) can cause aggregation of graphene sheets, resulting in a decreased specific area to 128.2 m^2 g^{-1}. In a further work, Choi et al. employed polystyrene colloidal particles as a template, which were subsequently removed with toluene [117]. This low-temperature solution technique avoids the restacking of graphene sheets and the collapse of porous structure. It also shows a good electrical conductivity
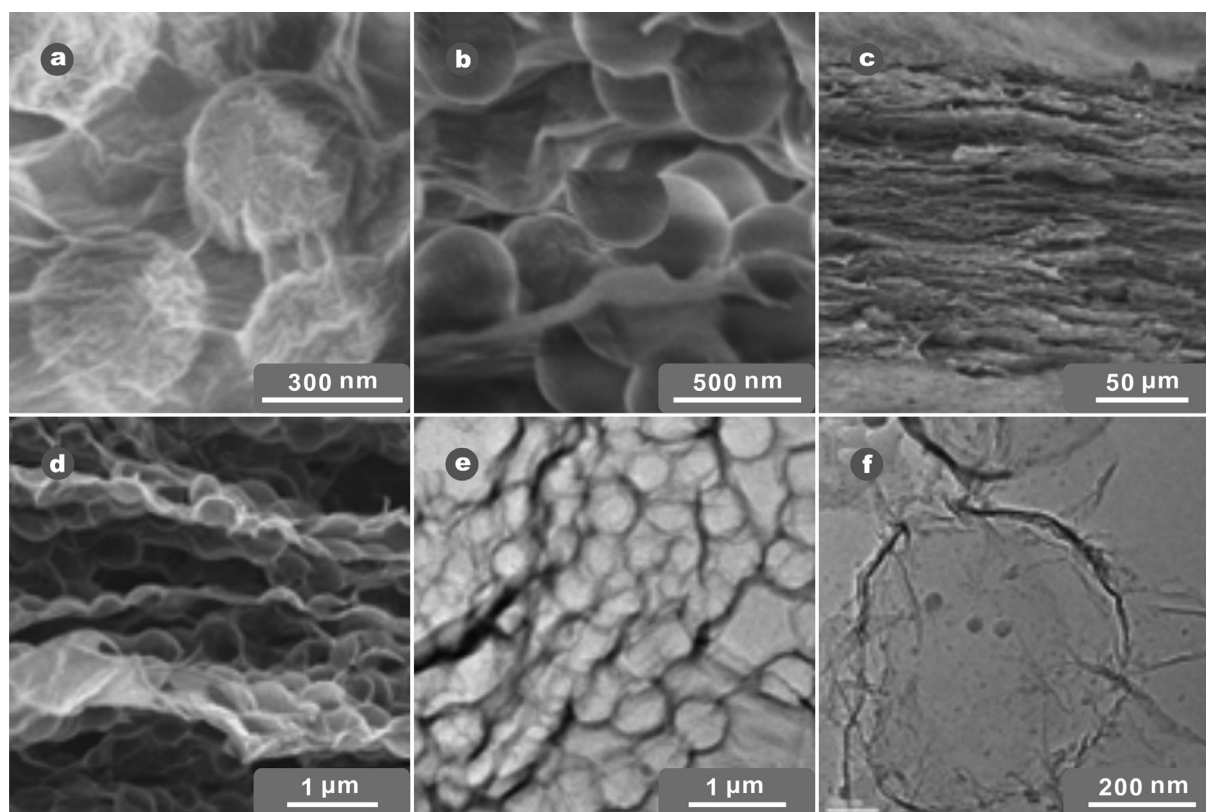

Fig. 7. SEM image of (a) surface, and (b) cross-section of a GO-PMMA composite film; (c) low and (d) high magnification SEM images of the cross-section of the MGF, (e) low and (f) high resolution TEM images of graphene bubbles within a MGF sample [144]. Copyright 2012, the Royal Society of Chemistry.

(1201 S m^{-1}). The hybrid electrode incorporating this 3D graphene foam as scaffold supports the growth of a thin layer of amorphous MnO_2 in to the graphene framework (see Fig. 8). The MnO_2-e-CMG nanocomposites with the large surface area and high conductivity of the interconnected 3D framework facilitate fast ionic transport show the superior electrochemical properties, *i.e.*, a capacitance value of 389 F g^{-1} at 1 A g^{-1}, 97.7% capacitance retention on a current increase to 35 A g^{-1}, an energy density of 44 W h kg^{-1} and a power density of 25 kW kg^{-1}, as asymmetric supercapacitors with a potential window of 2.0 V.

In the fabrication processes discussed above, the resultant graphene foams are of chemically reduced graphene oxides, which can include structural defects and chemical moieties introduced in the synthesis procedures [145]. Therefore, the electrical conductivity of the as-prepared graphene foams can be largely comprised. In addition to 3D graphene foams using polymer spheres as a sacrifice template, chemical vapor deposition (CVD) on Ni foam is also used as an efficient process to synthesize graphene foams, which can be seamlessly continuous and highly conductive with fewer defects for fabrication of monolithic 3D nanocomposite-type electrode. Zhang et al. prepared 3D graphene networks by using Ni foam as a sacrificial template by a facile CVD process with ethanol as a carbon source (see Fig. 9) [146]. The 3D graphene networks were superior templates for the construction of graphene-NiO 3D nanocomposites for supercapacitor electrodes. The high conductivity, which is almost comparable to that of the pristine graphene, and a great specific surface area can promote a rapid access of electrolyte ions to the NiO surface and facilitate the fast electron transport between the active materials and current collectors in supercapacitor. The NiO-graphene 3D nanocomposite has a high specific capacitance of ~816 F g^{-1} at the scanning rate of 5 mV s^{-1}, and a stable cycling performance without much degradation after 2000 cycles. Dong et al. designed nanocomposite materials, which incorporate Co_3O_4 nanowires into graphene foam, and the Co_3O_4 nanowires are assembled into 3D graphene foam and synthesized *via* chemical vapor deposition using nickel foam as sacrifice substrates [147]. This electrode material delivers a specific capacitance of ~1100 F g^{-1} at the current density of 10 A g^{-1} with an enhanced specific capacitance
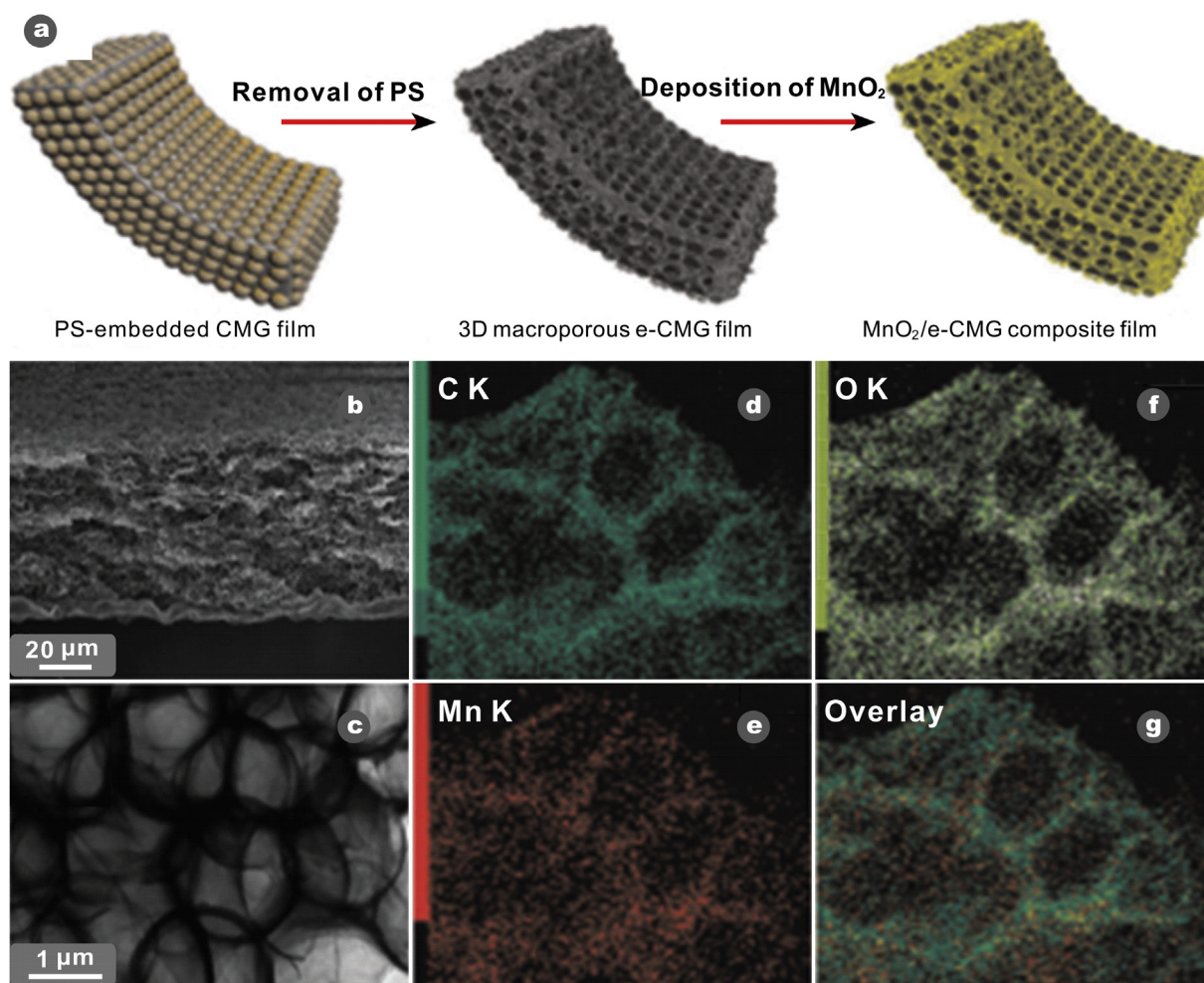

Fig. 8. (a) Schematic illustrating the fabrication of 3D macroporous MnO_2-chemically modified graphene films. (b) and (c) low-magnified cross-sectional SEM and TEM images of chemically modified graphene film. (d—g) EDS mapping of C, O, Mn and overlay elements on a segment of MnOs-chemically modified graphene film. Reproduced with permission [117]. Copyright 2012, American Chemical Society.

after 500 cycles. Xie et al. reported graphenne-MnO$_2$ 3D nanocomposite network developed by electrochemically depositing MnO$_2$ at a mass loading of 9.8 mg cm^{-2} (i.e., ~92.9% of the mass of the entire electrode) into 3D graphene using Ni foam as a template [148]. This flexible nanocomposite electrode shows an area capacitance of 1.42 F cm^{-2} at the scanning rate of 2 mV s^{-1} and a desired cycling ability, demonstrating that 3D graphene networks are an excellent supporter for active materials.

Graphene aerogels (GAs) and hydrogels are a novel class of ultralight and porous carbon-based materials exhibiting both high strength-to-weight and surface-area-to-volume ratios [149−151]. The 3D porous frameworks of GAs can provide multidimensional ion/electron transport pathways, offering easy access even to solid-state electrolytes, and minimize transport distances between bulk electrode and electrolytes [117,152−154]. These features enable GAs to be potentially used as additive/binder-free electrodes in electrochemical applications. Müllen et al. demonstrated a simplified prototype device of high-performance electrode materials based on 3D nitrogen and boron co-doped monolithic graphene aerogels (BN-GAs) developed by an one-step hydrothermal reduction process (see Fig. 10). The as-derived BN-GAs electrodes exhibit a specific capacitance of ~62 F g^{-1}, a good rate capability, an enhanced energy density of ~8.65 W h kg^{-1} and a power density of ~1600 W kg^{-1} [132]. Similarly, 3D self-assembled graphene hydrogel was prepared *via* chemical reduction of aqueous GO dispersions with sodium ascorbate. Shi et al. reported that the graphene hydrogel shows a well-defined and cross-linked 3D porous structure with pore sizes

ranging from sub-micrometers to micrometers and a high electrical conductivity [155]. The specific capacitance measured was ~240 F g^{-1} at a charge−discharge current density of 1.2 A g^{-1} in 1 M aqueous solution of H$_2$SO$_4$. Xu et al. reported a scalable approach to produce aqueous dispersions of holey graphene oxides (HGO) with abundant in-plane nanopores *via* a convenient mild defect-etching reaction approach. They found that the holey graphene oxides could function as a versatile building block for the assembly of macrostructures, *i.e.*, holey graphene hydrogels with 3D hierarchical porosity and improved specific surface areas. The holey graphene hydrogel (HGH) could be directly used as binder-free supercapacitor electrodes with a specific capacitance in the range of 283 F g^{-1} to 234 F g^{-1}, as well as excellent rate capability and cycling stability [156].

Certain polymers are incorporated into graphene aerogels. An et al., used multi-redox anthraquinone derivative alizarin (AZ) molecules to modify 3D self-assembled graphene hydrogels (SGHs) by a non-covalent functionalization process. The resultant AZ-SGHs hybrid electrodes show an excellent capacitive performance in terms of wide voltage window (i.e., 1.4 V in 1 mol L^{-1} H$_2$SO$_4$ solution), and a greater specific capacitance (i.e., 350 F g^{-1} at 1 A g^{-1}, which are two times greater than those of bare SGHs), and a high rate capability (i.e., specific capacitance at 200 A g^{-1} is 61% of that at 1 A g^{-1}). Noted that desirable self-synergy and potential self-matching behavior are achieved when the resultant AZ-SGHs electrodes are integrated into a symmetric supercapacitor. The integrated devices deliver a high energy density of 18.2 W h kg^{-1} at 700 W kg^{-1}, compared favorably to other
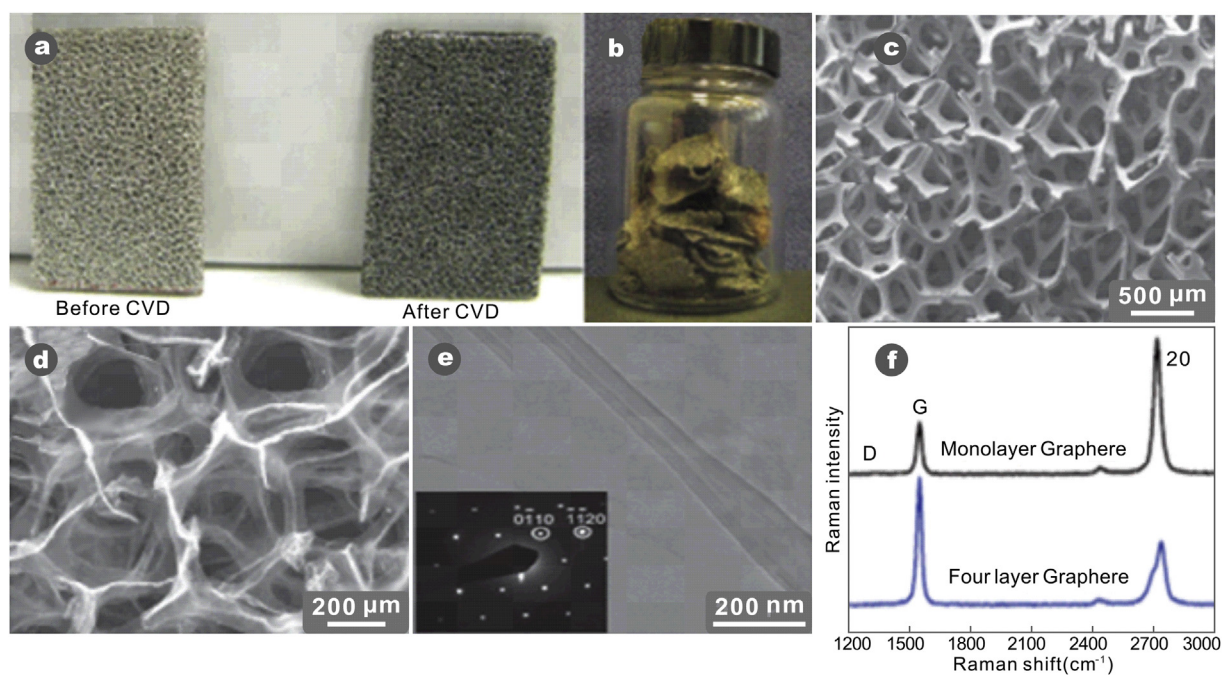

Fig. 9. Photographs of (a) Ni foam before and after the growth of graphene, and (b) 3D graphene networks obtained in a single CVD process after removal of the Ni foam. SEM images of (c) 3D graphene networks grown on Ni foam after CVD and (d) 3D graphene networks after removal of Ni foam. (e) TEM image of a graphene sheet. The inset shows the SAED pattern of graphene sheet. (f) Raman spectra of 3D graphene networks [146]. Copyright 2011, Wiley-VCH Verlag GmbH & Co. KGaA, Weinheim.
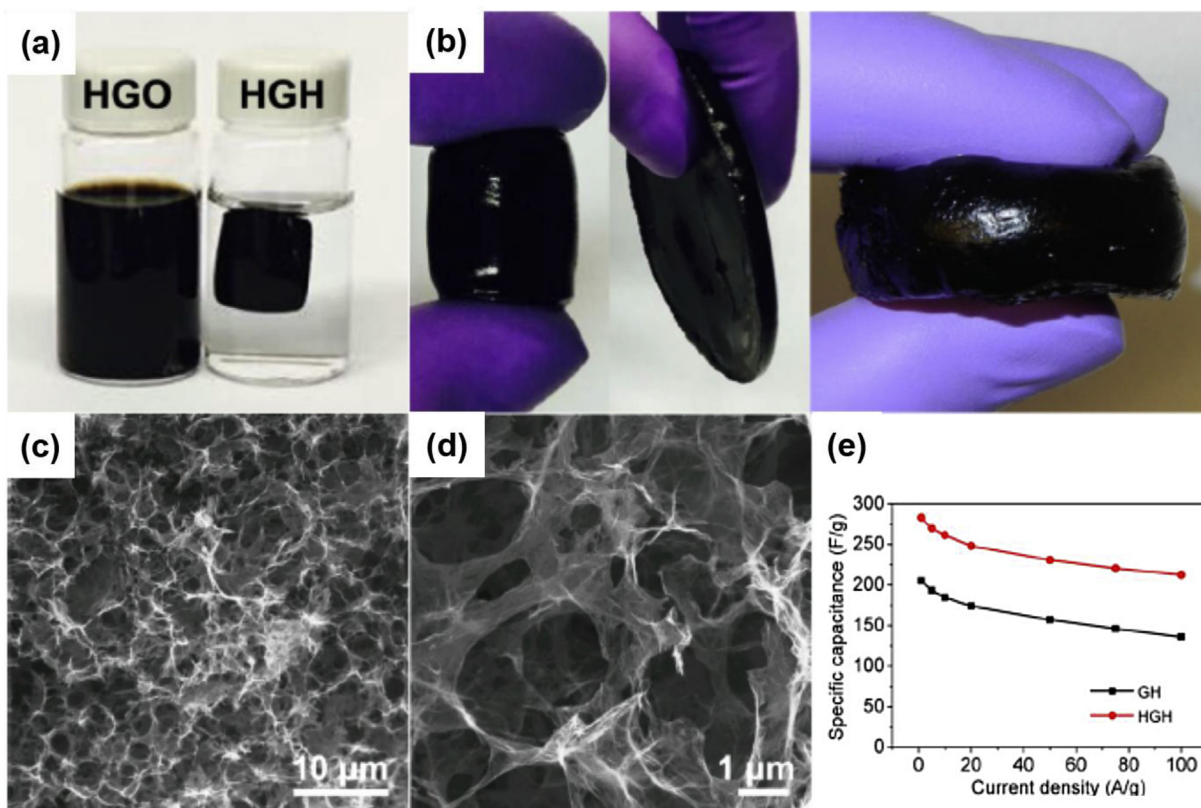
Fig. 10. Preparation and characterization of HGH. (a) Photographs of a HGO aqueous dispersion (2 mg/mL) and as-prepared HGH. (b) Photographs of a series of HGHs with different sizes and shapes. (c) Low- and (d) high-magnification SEM images of the interior microstructures of freeze-dried HGH. (e) Specific capacitances versus current densities [132]. Copyright 2015, American Chemical Society.

symmetric supercapacitors (<10 W h kg^{-1}) in aqueous electrolyte solutions, and exhibit an extraordinary rate capability with 64% of specific capacitance being retained when the current density increases from 1 to 50 A g^{-1} [157]. Chen et al. developed a novel type of electrode material with the unique structure of low-conductive electroactive polyhydroquinone (PHQ) being coated into a highly conductive three-dimensional (3D) porous graphene hydrogel (GHG). The 3D nanohybrid-type electrode materials were prepared via a one-step reaction between graphene oxide and hydroquinone under mild conditions. Due to the contribution of large specific capacitance of PHQ and 3D porous structure of GHG, the 3D nanohybrids electrode material showed a specific capacitance of 490 F g^{-1} at the current density of 24 A g^{-1} [158].

Although these bulk 3D graphene hydrogels can be facilely prepared by an one-step hydrothermal method, their inflexible structures and low mechanical strength restrict their applications as a flexible electrode [97]. Recently, Duan et al. demonstrated a free-standing holey graphene (HGF) framework developed via pressing bulk hydrogel into a high-density hydrogel film that is attached onto a flexible current collector. It was assembled into an all-solid-state flexible supercapacitor with polyvinyl alcohol (PVA) gel electrolyte [159]. The HGF electrode material was demonstrated with a gravimetric capacitance of 298 F g^{-1} and volumetric capacitance of 212 F cm^{-3} in organic electrolytes, and a stable capacitance retention of 87% after 10,000 cycles.

4. Conclusion and outlook

Graphene-based materials in different forms of 0D, 1D, 2D to 3D have proven to be excellent candidates of electrode materials in electrochemical energy storage systems, such as supercapacitors. In recent years, considerable efforts have been made on the structural design, material fabrication, performance evaluation, as well as understanding of the key electrochemical phenomena observed. To realize the expected full-scale practical application, the quality and reproducible quantity of the electrode materials both will have to be further improved, in particular with the development of the most desired structures tunable in nano-, micro-, meso- and macro-scales. The low cost and effective process to produce graphene-based materials is the chemical exfoliation of graphite into GO and the subsequent reasonable reduction of GO to rGO. However, before the large scale application of this facile processing method in electrochemical energy storage devices, the stabilization of single or few-layer graphene sheets in various solvents and the preservation of their intrinsic properties must be addressed in order to break the bottleneck of re-stacking of graphene sheets. This review summarized recent development on graphene-based materials for supercapacitor electrodes based on their structural complexity: zero-dimensional (0D) (e.g. free-standing graphene dots and particles), one-dimensional (1D) (e.g. fiber-type and yarn-type structures), two-dimensional (2D) (e.g. graphene-based

nanocomposites films and papers), and three-dimensional (3D) (e.g. graphene-based foams and hydrogels).

To fabricate supercapacitors with free-standing graphene particles, slurry casting method was generally employed, in which the active material powders were mixed with polymer binder and conductive additives to connect electrode material with current collectors. However, these polymers and the conductive additives generally make little contribution to the overall capacitance and decrease both the volumetric and gravimetric capacitance of electrodes. Compared to the free-standing graphene particles, supercapacitors made of 1D fiber-type or yarn-type and 2D graphene-based films as electrode can be made binder- and collector-free. These 1D and 2D structures possess a high electrical conductivity and a superior mechanical flexibility. However, the structures with moderate rate stability and power density are achieved due to the porous structure and varying degrees of graphene sheet aggregation, which can affect the effective diffusion of electrolyte ions. The interconnected graphene networks and tunable porous structure in varying scales, which can be achieved in 3D graphene foam/hydrogels, can lead to a better control in the restacking of graphene sheets, therefore having the improved rate and power performance, although their mechanical strength can be compromised.

To develop the graphene-based materials as supercapacitor electrodes and broaden their applications into other energy storage devices, the following future aspects should be considered:

(i) Graphene-based electrode materials with different architectures exhibit varying physical, mechanical and chemical behaviors, therefore affecting their performance in energy storage. Compared to the 0D, 1D and 2D structures, more attention should be paid to further exploring the tunable 3D graphene networks with interconnected porous structure, which can be manipulated for large internal surface area, ion/charge pathways, and avoiding the dead volume and collapse of the overall structures.

(ii) The nanocomposites consisting of graphene-based and pseudocapacitive materials, *i.e.*, those graphene/conductive polymers, graphene/metal oxides or hydroxides, are promising for achieving the long awaited requirement of both power density and high energy density. Therefore, there is a need to future explore efforts on the clarification of the nanohybrid structures and the control of the interfacial interaction between graphene and pseudocapacitive materials in order to improve the overall Faradic processes across the interface.

(iii) The rapid development of flexible electronics requires flexible and deformable energy storage devices. Therefore, future studies focus on the development of mechanical flexibility of graphene-based materials for supercapacitors and other energy storage devices.

(vi) The multifunctional or self-powered hybrid systems will be of considerable interests for future development.

Recent pioneer work on the combination of flexible supercapacitors with other electronic and energy devices (*i.e.*, solar cells, Li-ion batteries, electrochromic devices and nano-generators) were reported. Therefore, the integration of graphene-based supercapacitors with these devices will be of considerable values and a challenge as well.

Acknowledgment

References

[1] Miller JR, Simon P. Electrochemical capacitors for energy management. Science 2008;321:651−2.

[2] Simon P, Gogotsi Y. Materials for electrochemical capacitors. Nat Mater 2008;7:845−54.

[3] Liu C, Li F, Ma LP, Cheng HM. Advanced materials for energy storage. Adv Mater 2010;22:E28−62.

[4] Kaempgen M, Chan CK, Ma J, Cui Y, Gruner G. Printable thin film supercapacitors using single-walled carbon nanotubes. Nano Lett 2009;9:1872−6.

[5] Winter M, Brodd R. What are batteries, fuel cells, and supercapacitors. J Chem Rev 2004;104:4245−69.

[6] Shi W, Zhu J, Sim DH, Tay HH, Lu Z, Zhang X, et al. Achieving high specific charge capacitances in Fe_3O_4/reduced graphene oxide nanocomposites. J Mater Chem 2011;21:3422−7.

[7] Hu CC, Chang KH, Lin MC, Wu YT. Design and tailoring of the nanotubular arrayed architecture of hydrous RuO_2 for next generation supercapacitors. Nano Lett 2006;6:2690−5.

[8] Ke YK, Tsai YS, Huang YS. Electrochemical capacitors of RuO_2 nanophase grown on $LiNbO_3$ (100) and sapphire(0001) substrates. J Mater Chem 2005;15:2122−7.

[9] Xiao W, Xia H, Fuh JYH, Lu L. Growth of single-crystal α-MnO_2 nanotubes prepared by a hydrothermal route and their electrochemical properties. J Power Sources 2009;193:935−8.

[10] Xia JL, Chen F, Li JH, Tao NJ. Measurement of the quantum capacitance of graphene. Nat Nanotechnol 2009;4:505−9.

[11] Booth TJ, Blake P, Nair RR, Jiang D, Hill EW, Bangert U, et al. Macroscopic graphene membranes and their extraordinary stiffness. Nano Lett 2008;8:2442−6.

[12] Lee C, Wei XD, Kysar JW, Hone J. Measurement of the elastic properties and intrinsic strength of monolayer graphene. Science 2008;321:385−7.

[13] Liang JJ, Huang Y, Zhang L, Wang Y, Ma YF, Guo TY, et al. Molecular-level dispersion of graphene into poly(vinyl alcohol) and effective reinforcement of their nanocomposites. Adv Funct Mater 2009;19:2297−302.

[14] Huang X, Qi XY, Boey F, Zhang H. Graphene-based composites. Chem Soc Rev 2012;41:666−86.

[15] Kim KS, Zhao Y, Jang H, Lee SY, Kim JM, Kim KS, et al. Large-scale pattern growth of graphene films for stretchable transparent electrodes. Nature 2009;457:706−10.

[16] He QY, Wu SX, Gao S, Cao XH, Yin ZY, Li H, et al. Organic photovoltaic devices using highly flexible reduced graphene oxide films as transparent electrodes. ACS Nano 2010;4:5263−8.

[17] Schedin F, Geim AK, Morozov SV, Hill EW, Blake P, Katsnelson MI, et al. Detection of individual gas molecules adsorbed on graphene. Nat Mater 2007;6:652−5.

[18] He QY, Sudibya HG, Yin ZY, Wu SX, Li H, Boey F, et al. Centimeter-long and large-scale micropatterns of reduced graphene oxide films: fabrication and sensing applications. ACS Nano 2010;4:3201—8.

[19] Liang JJ, Xu YF, Huang Y, Zhang L, Wang Y, Ma YF, et al. Infrared-triggered actuators from graphene-based nanocomposites. J Phys Chem C 2009;113:9921—7.

[20] Park S, An J, Suk JW, Ruoff RS. Graphene-based actuators. Small 2010;6:10—212.

[21] Xie XJ, Qu LT, Zhou C, Li Y, Zhu J, Bai H, et al. An asymmetrically surface-modified graphene film electrochemical actuator. ACS Nano 2010;4:6050—4.

[22] Liang JJ, Huang Y, Oh J, Kozlov M, Sui D, Fang SL, et al. Electro-mechanical actuators based on graphene and graphene/Fe$_3$O$_4$ hybrid paper. Adv Funct Mater 2011;21:3778—84.

[23] Becerril HA, Mao J, Liu Z, Stoltenberg RM, Bao Z, Chen Y. Evaluation of solution-processed reduced graphene oxide films as transparent conductors. ACS Nano 2008;2:463—70.

[24] Brownson DAC, Kampouris DK, Banks CE. J Power Sources 2011;196:4873.

[25] Pumera M. Graphene-based nanomaterials and their electrochemistry. Chem Soc Rev 2010;39:4146—57.

[26] Zhang LL, Zhou R, Zhao XS. Graphene-based materials as super-capacitor electrode. J Mater Chem 2010;20:5983—92.

[27] Mitra S, Sampath S. Electrochemical capacitors based on exfoliated graphite electrodes batteries, fuel cells, and energy conversion. Electrochem Solid-State Lett 2004;7:A264—8.

[28] Wang X, Zhi LJ, Mullen K. Transparent, conductive graphene electrodes for dye-sensitized solar cells. Nano Lett 2008;8:323—7.

[29] Novoselov KS, Geim AK, Morozov SV, Jiang D, Zhang Y, Dubonos SV, et al. Electric field effect in atomically thin carbon films. Science 2004;306:666—9.

[30] Hernandez Y, Nicolosi V, Lotya M, Blighe FM, Sun Z, De S, et al. High-yield production of graphene by liquid-phase exfoliation of graphite. Nat Nanotechnol 2008;3:563—8.

[31] Tung VC, Allen MJ, Yang Y, Kaner RB. High-throughput solution processing of large-scale graphene. Nat Nanotechnol 2009;4:25—9.

[32] Stankovich S, Dikin DA, Dommett GHB, Kohlhaas KM, Zimney EJ, Stach EA, et al. Graphene-based composite materials. Nature 2006;442:282—6.

[33] Seredych M, Bandosz TJ. Removal of ammonia by graphite oxide via its intercalation and reactive adsorption. Carbon 2007;45:2130—2.

[34] Chen X, Chen X, Zhang F, Yang Z, Huang S. One-pot hydrothermal synthesis of reduced graphene oxide/carbon nanotube/α-Ni(OH)$_2$ composites for high performance electrochemical supercapacitor. J Power Sources 2013;243:555—61.

[35] Ke Q, Liu Y, Liu H, Zhang Y, Hu Y, Wang J. Surfactant-modified chemically reduced graphene oxide for electrochemical super-capacitors. RSC Adv 2014;4:26398—406.

[36] Zhang K, Zhang LL, Zhao XS, Wu J. Graphene/polyaniline nanofiber composites as supercapacitor electrodes. Chem Mater 2010;22:1392—401.

[37] Cai W, Piner RD, Stadermann FJ, Park S, Shaibat MA, Ishii Y, et al. Synthesis and solid-state NMR structural characterization of 13C-Labeled graphite oxide. Science 2008;321:1815—7.

[38] Cai Y, Zhang A, Feng YP, Zhang C. Switching and rectification of a single light-sensitive diarylethene molecule sandwiched between graphene nanoribbons. J Chem Phys 2011;135. 184703.

[39] Yu Q, Lian J, Siriponglert S, Li H, Chen YP, Pei SS. Graphene segregated on Ni surfaces and transferred to insulators. Appl Phys Lett 2008;93. 113103.

[40] Zhu Y, Murali S, Cai W, Li X, Suk JW, Potts JR, et al. Graphene and graphene oxide: synthesis, properties, and applications. Adv Mater 2010;22:3906—24.

[41] Dato A, Radmilovic V, Lee Z, Phillips J, Frenklach M. Substrate-free gas-phase synthesis of graphene sheets. Nano Lett 2008;8:2012—6.

[42] Wu Y, Wang B, Ma Y, Huang Y, Li N, Zhang F, et al. Efficient and large-scale synthesis of few-layered graphene using an arc-discharge method and conductivity studies of the resulting films. Nano Res 2010;3:661—9.

[43] Hirata M, Gotou T, Horiuchi S, Fujiwara M, Ohba M. Thin-film particles of graphite oxide 1:: high-yield synthesis and flexibility of the particles. Carbon 2004;42:2929—37.

[44] Stoller MD, Park S, Zhu Y, An J, Ruoff RS. Graphene-based ultra-capacitors. Nano Lett 2008;8:3498—502.

[45] Gao W, Alemany LB, Ci LJ, Ajayan PM. New insights into the structure and reduction of graphite oxide. Nat Chem 2009;1:403—8.

[46] Zhu C, Guo S, Fang Y, Dong S. Reducing sugar: new functional molecules or the green synthesis of graphene nanosheets. ACS Nano 2010;4:429—37.

[47] Zhang J, Yang H, Shen G, Cheng P, Zhang J, Guo S. Reduction of graphene oxide via L-ascorbic acid. Chem Comm 2010;46:1112—4.

[48] Merino MJ, Guardia L, Paredes JI, Rodil SV, Fernandez PS, Alonso AM, et al. Vitamin C is an ideal substitute for hydrazine in the reduction of graphene oxide suspensions. J Phys Chem C 2010;114:6426—32.

[49] Gao J, Liu F, Liu Y, Ma N, Wang Z, Zhang X. Environment-friendly method to produce graphene that employs vitamin C and amino acid. Chem Mater 2010;22:2213—8.

[50] Akhavan O, Ghaderi E, Aghayee S, Fereydooni Y, Talebi A. The use of a glucose-reduced graphene oxide suspension for photothermal cancer therapy. J Mater Chem 2012;22:13773—81.

[51] Liu J, Fu S, Yuan B, Li Y, Deng Z. Toward a universal "adhesive nanosheet" for the assembly of multiple nanoparticles based on a protein induced reduction/decoration of graphene oxide. J Am Chem Soc 2010;132:7279—81.

[52] Akhavan O, Kalaee M, Alavi ZS, Ghiasi SMA, Esfandiar A. Increasing the antioxidant activity of green tea polyphenols in the presence of iron for the reduction of graphene oxide. Carbon 2012;50:3015—25.

[53] Akhavan O, Ghaderi E. Escherichia coli bacteria reduce graphene oxide to bactericidal graphene in a self-limiting manner. Carbon 2012;50:1853—60.

[54] Salas EC, Sun Z, Luttge A, Tour JM. Reduction of graphene oxide via bacterial respiration. ACS Nano 2010;4:4852—6.

[55] Cote LJ, Silva RC, Huang J. Flash reduction and patterning of graphite oxide and its polymer composite. J Am Chem Soc 2009;131:11027—32.

[56] Zhou Y, Bao Q, Ai L, Tang L, Zhong Y, Loh KP. Hydrothermal dehydration for the "green" reduction of exfoliated graphene oxide to graphene and demonstration of tunable optical limiting properties. Chem Mater 2009;21:2950—6.

[57] Ai K, Liu Y, Lu L, Cheng X, Huo L. A novel strategy for making soluble reduced graphene oxide sheets cheaply by adopting an endogenous reducing agent. J Mater Chem 2011;21:3365—70.

[58] Xu C, Wang X, Zhu J. Graphene metal particle nanocomposites. J Phys Chem C 2008;112:19841—5.

[59] Akhavan O, Ghaderi E. Photocatalytic reduction of graphene oxide nanosheets on TiO$_2$ thin film for photoinactivation of bacteria in solar light irradiation. J Phys Chem C 2009;113:20214—20.

[60] Williams G, Seger B, Kamat PV. TiO$_2$-graphene nanocomposites UV assisted photocatalytic reduction of graphene oxide. ACS Nano 2008;2:1487—91.

[61] Akhavan O, Abdolahad M, Esfandiar A, Mohatashamifar M. Photo-degradation of graphene oxide sheets by TiO$_2$ nanoparticles after a photocatalytic reduction. J Phys Chem C 2010;114:12955—9.

[62] Akhavan O. Graphene nanomesh by ZnO nanorod photocatalysts. ACS Nano 2010;4:4174—80.

[63] Akhavan O, Choobtashani M, Ghaderi E. Protein degradation and RNA efflux of viruses photocatalyzed by graphene-tungsten oxide composite under visible light irradiation. J Phys Chem C 2012;116:9653—965.

[64] Byon HR, Lee SW, Chen S, Hammond PT, Shao-Horn Y. Thin films of carbon nanotubes and chemically reduced graphenes for electro-chemical micro-capacitors. Carbon 2011;49:457—67.

[65] Zhang K, Mao L, Zhang LL, Chan HSO, Zhao XS, Wu J. Surfactant-intercalated, chemically reduced graphene oxide for high performance supercapacitor electrodes. J Mater Chem 2011;21:7302—7.

[66] Mao L, Zhang K, Chan HSO, Wu J. Surfactant-stabilized graphene/polyaniline nanofiber composites for high performance supercapacitor electrode. J Mater Chem 2012;22:80—5.

[67] Liang C, Li Z, Dai S. Mesoporous carbon materials: synthesis and modification. Angew Chem Int Ed 2008;47:3696—717.

[68] Lai L, Huang G, Wang X, Weng J. Solvothermal syntheses of hollow carbon microspheres modified with -NH$_2$ and -OH groups in one-step process. Carbon 2010;48:3145—56.

[69] Yang ZC, Tang CH, Gong H, Li X, Wang J. Hollow spheres of nanocarbon and their manganese dioxide hybrids derived from soft template for supercapacitor application. J Power Sources 2013;240:713—20.

[70] Cai Y, Zhang G, Zhang YW. Polarity-reversed robust carrier mobility in monolayer MoS$_2$ nanoribbons. J Am Chem Soc 2014;136:6269—75.

[71] Cai Y, Ke Q, Zhang G, Zhang YW. Energetics, charge transfer and magnetism of small molecules physisorbed on phosphorene. J Phys Chem C 2015;119:3102—10.

[72] Stenger-Smith JD, Webber CK, Anderson N, Chafin AP, Zong KK, Reynolds JR. Poly(3,4-alkylenedioxythiophene)-based supercapacitors using ionic liquids as supporting electrolytes. J Electrochem Soc 2002;149:A973—7.

[73] Frackowiak E, Khomenko V, Jurewicz K, Lota K, Beguin F. Supercapacitors based on conducting polymers/nanotubes composites. J Power Sources 2006;153:413—8.

[74] Kötz R, Carlen M. Principles and applications of electrochemical capacitors. Electrochim Acta 2000;45:2483—98.

[75] Cottineau T, Toupin M, Delahaye T, Brousse T, Belanger D. Nanostructured transition metal oxides for aqueous hybrid electrochemical supercapacitors. Appl Phys A Mater Sci Process 2006;82:599—606.

[76] Du X, Wang CY, Chen MM, Jiao Y, Wang J. Electrochemical performances of nanoparticle Fe$_3$O$_4$/activated carbon supercapacitor using KOH electrolyte solution. J Phys Chem C 2009;113. 2643.

[77] Chen S, Zhu J, Wu X, Han Q, Wang X. Graphene oxide-MnO$_2$ nanocomposites for supercapacitors. ACS Nano 2010;4:2822—30.

[78] Wu ZS, Ren W, Wang DW, Li F, Liu B, Cheng HM. High-energy MnO$_2$ nanowire/graphene and graphene asymmetric electrochemical capacitors. ACS Nano 2010;4:5835—42.

[79] Chen S, Zhu J, Wang X. From graphene to metal oxide nanolamellas: a phenomenon of morphology transmission. ACS Nano 2010;4:6212—8.

[80] Yan J, Fan Z, Wei T, Qian W, Zhang M, Wei F. Fast and reversible surface redox reaction of graphene-MnO$_2$ composites as supercapacitor electrodes. Carbon 2010;48:3825—33.

[81] Li Z, Wang J, Liu S, Liu X, Yang S. Synthesis of hydrothermally reduced graphene/MnO$_2$ composites and their electrochemical properties as supercapacitors. J Power Sources 2011;196:8160—5.

[82] Wang H, Casalongue HS, Liang Y, Dai H. Ni(OH)$_2$ nanoplates grown on graphene as advanced electrochemical pseudocapacitor materials. J Am Chem Soc 2010;132:7472—7.

[83] Wang H-W, Hu Z-A, Chang Y-Q, Chen Y-L, Zhang Z-Y, Yang Y-Y, et al. Preparation of reduced graphene oxide/cobalt oxide composites and their enhanced capacitive behaviors by homogeneous incorporation of reduced graphene oxide sheets in cobalt oxide matrix. Mater Chem Phys 2011;130:672—9.

[84] Ke Q, Tang C, Liu Y, Liu H, Wang J. Intercalating graphene with clusters of Fe$_3$O$_4$ nanocrystals for electrochemical supercapacitors. Mater Res Express 2014;1. 025015.

[85] Lee JS, Kim SI, Yoon JC, Jang JH. Chemical vapor deposition of mesoporous graphene nanoballs for supercapacitor. Acs Nano 2013;7:6047—55.

[86] Yoon M, Choi WM, Baik H, Shin HJ, Song I, Kwon MS, et al. Synthesis of multilayer graphene balls by carbon segregation from nickel nanoparticles. ACS Nano 2012;6:6803—11.

[87] Park SH, Kim HK, Yoon SB, Lee CW, Ahn D, Lee SI, et al. Spray-assisted deep-frying process for the in situ spherical assembly of graphene for energy-storage devices. Chem Mater 2015;27:457—65.

[88] Meng Y, Zhao Y, Hu C, Cheng H, Hu Y, Zhang Z, et al. Graphene core-sheath microfibres for all-solid-state, stretchable fibriform

[89] Ren J, Bai W, Guan G, Zhang Y, Peng H. Flexible and weaveable capacitor wire based on a carbon nanocomposite fiber. Adv Mater 2013;25:5965—70.

[90] Ren J, Li L, Chen C, Chen X, Cai Z, Qiu L, et al. Twisting carbon nanotube fibres for both wire-shaped microsupercapacitor and microbattery. Adv Mater 2013;25:1155—9.

[91] Tao J, Liu N, Ma W, Ding L, Li L, Su J, et al. Solid-state high performance flexible supercapacitors based on polypyrrole-MnO$_2$-carbon fibre hybrid structure. Sci Rep 2013;3. 2286.

[92] Lee JA, Shin MK, Kim SH, Cho HU, Spinks GM, Wallace GG, et al. Ultrafast charge and discharge biscrolled yarn supercapacitors for textiles and microdevices. Nat Commun 2013;4. 1970.

[93] Kou L, Huang T, Zheng B, Han Y, Zhao X, Gopalsamy K, et al. Coaxial wet-spun yarn supercapacitors for high-energy density and safe wearable electronics. Nat Commun 2014;5. 3754.

[94] Cheng H, Dong Z, Hu C, Zhao Y, Hu Y, Qu L, et al. Textile electrodes woven by carbon nanotube-graphene hybrid fibers for flexible electrochemical capacitors. Nanoscale 2013;5:3428—34.

[95] Wang X, Liu B, Liu R, Wang Q, Hou X, Chen D, et al. Fiber-based flexible all-solid-state asymmetric supercapacitors for integrated photodetecting system. Angew Chem, Int Ed 2014;53:1849—53.

[96] Aboutalebi SH, Jalili R, Esrafilzadeh D, Salari M, Gholamvand Z, Yamin SA, et al. High-performance multifunctional graphene yarns: toward wearable all-carbon energy storage textiles. ACS Nano 2014;8:2456—66.

[97] Liu L, Yu Y, Yan C, Li K, Zheng Z. Wearable energy-dense and power-dense supercapacitor yarns enabled by scalable graphene-metallic textile composite electrodes. Nature Commun, http://dx.doi.org/10.1038/ncomms8260.

[98] Shao Y, El-Kady MF, Wang LJ, Zhang Q, Li Y, Wang H, Mousaviae MF, Kaner RB. Graphene-based materials for flexible supercapacitors. Chem. Soc. Rev http://dx.doi.org/10.1039/c4cs00316k.

[99] Günes F, Shin HJ, Biswas C, Han GH, Kim ES, Chae SJ, et al. Layer-by-layer doping of few-layer graphene film. ACS Nano 2010;4:4595—600.

[100] Gan S, Zhong L, Wu T, Han D, Zhang J, Ulstrup J, et al. Spontaneous and fast growth of large-area graphene nanofilms facilitated by oil/water interfaces. Adv Mater 2012;24:3958—64.

[101] Li D, Muller MB, Gilje S, Kaner RB, Wallace GG. Processable aqueous dispersions of graphene nanosheets. Nat Nanotechnol 2008;3:101—5.

[102] Yang X, Cheng C, Wang Y, Qiu L, Li D. Liquid-mediated dense integration of graphene materials for compact capacitive energy storage. Science 2013;341:534.

[103] Cai Y, Ke Q, Zhang G, Feng YP, Vivek BS, Zhang YW. Giant phononic anisotropy and unusual anharmonicity of phosphorene: interlayer coupling and strain Engineering. Adv Funct Mater 2015;25:2230—6.

[104] Cai Y, Zhang G, Zhang YW. Layer-dependent band alignment and work function of few-layer phosphorene. Sci Rep 2014;4. 6677.

[105] Lei Z, Christov N, Zhao XS. Intercalation of mesoporous carbon spheres between reduced graphene oxide sheets for preparing high-rate supercapacitor electrodes. Energy Environ Sci 2011;4:1866—73.

[106] Vickery JL, Patil AJ, Mann S. Fabrication of graphene-polymer nanocomposites with higher-order three-dimensional architectures. Adv Mater 2009;21:2180—4.

[107] Liu C, Yu Z, Neff D, Zhamu A, Jang BZ. Graphene-based supercapacitor with an ultrahigh energy density. Nano Lett 2010;10:4863—8.

[108] Wang GK, Sun X, Lu FY, Sun HT, Yu MP, Jiang WL, et al. Flexible pillared graphene-paper electrodes for high-performance electrochemical supercapacitors. Small 2012;8:452—9.

[109] Qiu L, Yang X, Gou X, Yang W, Ma ZF, Wallace GG, et al. Dispersing carbon nanotubes with graphene oxide in water and synergistic effects between graphene derivatives. Chem Eur J 2010;16:10653—8.

[110] Si Y, Samulski ET. Exfoliated graphene separated by platinum nanoparticles. Chem Mater 2008;20:6792—7.

[111] Li S, Luo Y, Lv W, Yu W, Wu S, Hou P, et al. Adv Energy Mater 2011;1:486—90.

[112] Paek SM, Yoo E, Honma I. Enhanced cyclic performance and lithium storage capacity of SnO$_2$/graphene nanoporous electrodes with three-dimensionally delaminated flexible structure. Nano Lett 2009;9:72–5.

[113] Burke A. Ultracapacitors: why, how, and where is the technology. J Power Sources 2000;91:37–50.

[114] Li YZ, Zhao X, Xu Q, Zhang QH, Chen D. Facile preparation and enhanced capacitance of the polyaniline sodium alginate nanofiber network for supercapacitors. J Langmuir 2011;27:6458–63.

[115] Fan LZ, Maier J. High-performance polypyrrole electrode materials for redox supercapacitors. Electrochem Commun 2006;8:937–40.

[116] Li M, Tang Z, Leng M, Xue J. Flexible solid-state supercapacitor based on graphene-based hybrid films. Adv Funct Mater 2014;24:7495–502.

[117] Choi BG, Yang M, Hong WH, Choi JW, Huh YS. 3D macroporous graphene frameworks for supercapacitors with high energy and power densities. ACS Nano 2012;6:4020–8.

[118] Yang M, Lee KG, Lee SJ, Lee SB, Y-K Han, Choi BG. Three-dimensional expanded graphene–metal oxide film via solid-state microwave irradiation for aqueous asymmetric supercapacitors. ACS Appl Mater Interfaces 2015;7:22364–71.

[119] Yang X, Zhu J, Qiu L, Li D. Bioinspired effective prevention of restacking in multilayered graphene films: towards the next generation of high-performance supercapacitors. Adv Mater 2011;3:2833–8.

[120] Choi BG, Hong J, Hong WH, Hammond PT, Park H. Facilitated ion transport in all-solid-state flexible supercapacitors. ACS Nano 2011;5:7205–13.

[121] Murugan AV, Muraliganth T, Manthiram A. Chem Mater 2009;21:5004–6.

[122] Zhang Y, Li H, Pan L, Lu T, Sun Z. Capacitive behavior of graphene-ZnO composite film for supercapacitors. J Electroanal Chem 2009;634:68–71.

[123] Wang DW, Li F, Zhao J, Ren W, Chen ZG, Tan J, et al. Fabrication of graphene/polyaniline composite paper via in situ anodic electropolymerization for high-performance flexible electrode. ACS Nano 2009;3:1745–52.

[124] Meng Y, Wang K, Zhang Y, Wei Z. Hierarchical porous graphene/polyaniline composite film with superior rate performance for flexible supercapacitors. Adv Mater 2013;25:6985–90.

[125] Yan J, Wei T, Shao B, Fan Z, Qian W, Zhang M, et al. Preparation of a graphene nanosheet/polyaniline composite with high specific capacitance. Carbon 2010;48:487–93.

[126] Zhang J, Yu Y, Liu L, Wu Y. Graphene-hollow PPy sphere 3D-nano-architecture with enhanced electrochemical performance. Nanoscale 2013;5:3052–7.

[127] Wang S, Ma L, Gan M, Fu S, Dai W, Zhou T, et al. Free-standing 3D graphene/polyaniline composite film electrodes for high-performance supercapacitors. J Power Sources 2015;299:347–55.

[128] Groenendaal L, Jonas F, Freitag D, Pielartzik H, Reynolds JR. Poly(3,4-ethylenedioxythiophene) and its derivatives: past, present, and future. Adv Mater 2000;12:481–94.

[129] Groenendaal L, Zotti G, Aubert PH, Waybright SM, Reynolds JR. Electrochemistry of poly(3,4-alkylenedioxythiophene) derivatives. Adv Mater 2003;15:855–79.

[130] Lehtimaki S, Suominen M, Damlin P, Tuukkanen S, Kvarnstrom C, Lupo D. Preparation of supercapacitors on flexible substrates with electrodeposited PEDOT/graphene composites. ACS Appl Mater Interfaces 2015;7:22137–47.

[131] Sun Y, Wu Q, Shi G. Graphene based new energy materials. Energy Environ Sci 2011;4:1113–32.

[132] Cong HP, Ren XC, Wang P, Yu SH. Macroscopic multifunctional graphene-based hydrogels and aerogels by a metal ion induced self-assembly process. ACS Nano 2012;6:2693–703.

[133] Wu ZS, Winter A, Chen L, Sun Y, Turchanin A, Feng X, et al. Three-dimensional nitrogen and boron co-doped graphene for high-performance all-solid-state supercapacitors. Adv Mater 2012;24:5130–5.

[134] Chen J, Sheng K, Luo P, Li C, Shi G. Graphene hydrogels deposited in nickel foams for high-rate electrochemical capacitors. Adv Mater 2012;24:4569–73.

[135] Chen W, Yan L. Centimeter-sized dried foam films of graphene: preparation, mechanical and electronic properties. Adv Mater 2012;24:6229–33.

[136] Meng C, Liu C, Chen L, Hu C, Fan S. Highly flexible and all-solid-state paper like polymer supercapacitors. Nano Lett 2010;10:4025–31.

[137] Chen H, Müller MB, Gilmore KJ, Wallace GG, Li D. Mechanically strong, electrically conductive, and biocompatible graphene paper. Adv Mater 2008;20:3557–61.

[138] Kim J, Cote LJ, Kim F, Yuan W, Shull KR, Huang JX. Graphene oxide sheets at interfaces. J Am Chem Soc 2010;132:8180–6.

[139] Tung VC, Kim J, Cote LJ, Huang JX. Sticky interconnect for solution-processed tandem solar cells. J Am Chem Soc 2011;133:9262–5.

[140] Yin SY, Zhang YY, Kong JH, Zou CJ, Li CM, Lu XH, et al. Assembly of graphene sheets into hierarchical structures for high-performance energy storage. ACS Nano 2011;5:3831–8.

[141] Liu F, Seo TS. A controllable self-assembly method for large-scale synthesis of graphene sponges and free-standing graphene films. Adv Funct Mater 2010;20:1930–6.

[142] Tang LH, Wang Y, Li YM, Feng HB, Lu J, Li JH. Preparation, structure, and electrochemical properties of reduced graphene sheet films. Adv Funct Mater 2009;19:2782–9.

[143] Biswas S, Drzal LT. Multilayered nano-architecture of variable sized graphene nanosheets for enhanced supercapacitor electrode performance. ACS Appl Mater Interfaces 2010;2:2293–300.

[144] Chen CM, Zhang Q, Huang CH, Zhao XC, Zhang BS, Kong QQ, et al. Macroporous 'bubble' graphene film via template-directed ordered-assembly for high rate supercapacitors. Chem Commun 2012;48:7149–51.

[145] Cai Y, Zhang A, Feng YP, Zhang C. Switching and rectification of a single light-sensitive diarylethene molecule sandwiched between graphene nanoribbon. J Chem Phys 2011;135:184703.

[146] Cao X, Shi Y, Shi W, Lu G, Huang X, Yan Q, et al. Preparation of novel 3D graphene networks for supercapacitor applications. Small 2011;7:316–3168.

[147] Dong XC, Xu H, Wang XW, Huang YX, Chan-Park MB, Zhang H, et al. 3D graphene–cobalt oxide electrode for high-performance super-capacitor and enzymeless glucose detection. ACS Nano 2012;6:3206–13.

[148] He Y, Chen W, Li X, Zhang Z, Fu J, Zhao C, et al. Freestanding three-dimensional graphene/MnO$_2$ composite networks as ultralight and flexible supercapacitor electrodes. ACS Nano 2012;7:174–82.

[149] Worsley MA, Pauzauskie PJ, Olson TY, Biener J, Satcher JH, Baumann TF. Synthesis of graphene aerogel with high electrical conductivity. J Am Chem Soc 2010;132:14067–9.

[150] Li D, Yang XW, Qiu L, Cheng C, Wu YZ, Ma ZF. Ordered gelation of chemically converted graphene for next-generation electroconductive hydrogel films. Angew Chem Int Ed 2011;50:7325–8.

[151] Tang ZH, Shen SL, Zhuang J, Wang X. Noble-metal-promoted three-dimensional macro assembly of single-layered graphene oxide. Angew Chem Int Ed 2010;49:4603–7.

[152] Sheng KX, Sun YQ, Li C, Yuan WJ, Shi GQ. Ultrahigh-rate supercapacitors based on eletrochemically reduced graphene oxide for ac line-filtering. Sci Rep 2012;2:247.

[153] Wu Q, Sun YQ, Bai H, Shi GQ. High-performance supercapacitor electrodes based on graphene hydrogels modified with 2-amino-anthraquinone moieties. Phys Chem Chem Phys 2011;13:11193–8.

[154] Zhang L, Shi GQ. Preparation of highly conductive graphene hydrogels for fabricating supercapacitors with high rate capability. J Phys Chem C 2011;115:17206–12.

[155] Xu Y, Sheng K, Li C, Shi G. Self-assembled graphene hydrogel via a one-step hydrothermal process. ACS Nano 2010;4:4324–30.

[156] Xu Y, Chen C, Zhao Z, Lin Z, Lee C, Xu X, et al. Duan, solution processable holey graphene oxide and its derived macrostructures for high-performance supercapacitors. Nano Lett 2015;15:4605–10.

[157] An N, An Y, Hu Z, Guo B, Yang Y, Lei Z. Graphene hydrogels non-covalently functionalized with alizarin: an ideal electrode material for symmetric supercapacitors. J Mater Chem A 2015;3:22239—46.

[158] Chen L, Wu J, Zhang A, Zhou A, Huang Z, Bai H, et al. One-step synthesis of polyhydroquinone-graphene hydrogel composites for high performance supercapacitors. J Mater Chem A 2015;3:16033—9.

[159] Xu Y, Lin Z, Huang X, Wang Y, Huang Y, Duan X. Functionalized graphene hydrogel-based high-performance supercapacitors. Adv Mater 2013;25:5779—84.
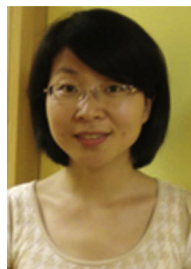
Qingqing KE, National University of Singapore. Email: msekq2001@gmail.com. Qingqing KE is a research fellow of Department of Materials Science and Engineering, National University of Singapore, Singapore. She has been doing post Doc. studies in Singapore since 2012. Her recent research focuses on graphene-based materials for supercapacitor electrodes.